Earth-Science Reviews xxx (2009) xxx–xxx

Contents lists available at ScienceDirect

Earth-Science Reviews

journal homepage: www.elsevier.com/locate/earscirev

Temporal and geochemical evolution of the Cenozoic intraplate volcanism of Zealandia

Christian Timm [a,*], Kaj Hoernle [a], Reinhard Werner [a], Folkmar Hauff [a], Paul van den Bogaard [a], James White [b], Nick Mortimer [c], Dieter Garbe-Schönberg [d]

[a] IFM-GEOMAR, Wischhofstr. 1-3, 24148 Kiel, Germany
[b] Geology Department, University of Otago, PO Box 56, Dunedin 9015, New Zealand
[c] GNS Science, Private Bag 1930, Dunedin, New Zealand
[d] Institut für Geowissenschaften, Christian Albrechts University of Kiel, Ludewig-Meyn-Strasse 10, 24118 Kiel, Germany

ARTICLE INFO

Article history:
Received 1 July 2008
Accepted 1 October 2009
Available online xxxx

Keywords:
intraplate volcanism
Zealandia
$^{40}Ar/^{39}Ar$ age dating
geochemistry
lithospheric removal
mantle plume

ABSTRACT

In order to constrain better the distribution, age, geochemistry and origin of widespread Cenozoic intraplate volcanism on Zealandia, the New Zealand micro-continent, we report new $^{40}Ar/^{39}Ar$ and geochemical (major and trace element and Sr–Nd–Hf–Pb isotope) data from offshore (Chatham Rise, Campbell and Challenger Plateaus) and onland (North, South, Auckland, Campbell, Chatham and Antipodes Islands of New Zealand) volcanism on Zealandia. The samples include nephelinite, basanite through phonolite, alkali basalt through trachyte/rhyolite, and minor tholeiite and basaltic andesite, all of which have ocean island basalt (OIB)-type trace element signatures and which range in age from 64.8 to 0.17 Ma. Isotope ratios show a wide range in composition ($^{87}Sr/^{86}Sr = 0.7027–0.7050$, $^{143}Nd/^{144}Nd = 0.5128–0.5131$, $^{177}Hf/^{176}Hf = 0.2829–0.2831$, $^{206}Pb/^{204}Pb = 18.62–20.67$, $^{207}Pb/^{204}Pb = 15.54–15.72$ and $^{208}Pb/^{204}Pb = 38.27–40.34$) with samples plotting between mid-ocean-ridge basalts (MORB) and Cretaceous New Zealand intraplate volcanic rocks.

Major characteristics of Zealandia's Cenozoic volcanism include longevity, irregular distribution and lack of age progressions in the direction of plate motion, or indeed any systematic temporal or spatial geochemical variations. We believe that these characteristics can be best explained in the context of lithospheric detachment, which causes upwelling and melting of the upper asthenospheric mantle and portions of the removed lithosphere. We propose that a large-scale seismic low-velocity anomaly, that stretches from beneath West Antarctica to Zealandia at a depth of >600 km may represent a geochemical reservoir that has been in existence since the Cretaceous, and has been supplying the upper mantle beneath Zealandia with HIMU-type plume material throughout the Cenozoic. In addition, the sources of the Cenozoic intraplate volcanism may be at least partially derived through melting of locally detached Zealandia lower lithosphere.

Contents

* Corresponding author. Tel.: +49 431 600 2141.
E-mail address: ctimm@ifm-geomar.de (C. Timm).

0012-8252/$ – see front matter © 2009 Elsevier B.V. All rights reserved.
doi:10.1016/j.earscirev.2009.10.002

1. Introduction

The origin of intraplate volcanism is a subject of intense debate at present. For continental areas, the classic models for explaining intraplate volcanism either invoke mantle plumes (e.g. Morgan, 1971) or extensive lithospheric thinning often preceding continental rifting (e.g. Weaver and Smith, 1989). Neither of these models however can adequately explain intraplate volcanism on the SW Pacific micro-continent of Zealandia (e.g. Finn et al., 2005; Panter et al., 2006; Hoernle et al., 2006; Sprung et al., 2007; Timm et al., 2009). Newer models for Zealandia volcanism can be divided into two groups: low-degree melting of lithosphere metasomatized by earlier subduction and plume-related processes (Finn et al., 2005; Panter et al., 2006; Sprung et al., 2007), or lithospheric removal (detachment) that results in asthenospheric upwelling and melting (Hoernle et al., 2006; Timm et al., 2009). The previous studies were largely based on geochemical results from subaerial samples from Zealandia, yet 90% of Zealandia is located beneath sea level. Here we present new $^{40}Ar/^{39}Ar$ age and comprehensive geochemical (major and trace element and Sr–Nd–Hf–Pb isotope) data from both subaerial and submarine parts of Zealandia. These include submarine samples obtained during RV Sonne SO168 and SO169 cruises from the Challenger and Campbell Plateaus and the Chatham Rise, and onland samples from the North, South, Chatham, and Subantarctic islands. In this paper we combine our spatially more comprehensive data set with data from the literature, in order to evaluate the temporal and spatial evolution of volcanism on Zealandia, to test existing models and to propose a new model for the origin of this widespread, long-lived and enigmatic intraplate volcanism.

2. Geodynamic background of Zealandia since the Late Cretaceous

The largely submerged continent of Zealandia covers an area of more than two million square kilometers and lies between ~25°–56°S and 160°E–168°W on the Pacific and Australian plates (Mortimer, 2004) (Fig. 1). The submerged parts of Zealandia consist of the Campbell Plateau in the southeast, the Bounty Trough, and Chatham Rise in the east and the Challenger Plateau and Lord Howe Rise in the northwest. The North and South Island of New Zealand, four groups of Subantarctic islands (Antipodes, Auckland, Campbell and Chatham Islands) and New Caledonia are the only emergent parts of Zealandia.

Before ~84 million years ago, Zealandia formed a part of the Gondwana super-continent, and was situated at its active eastern margin facing subducting proto-Pacific basin plates (e.g. Storey et al., 1999; Mortimer et al., 2006). Marine magnetic and satellite-derived gravity data indicate that the eastern and southeastern margins of the Chatham Rise and the Campbell Plateau were attached to the northern margin of Marie Byrd Land (West Antarctica) (e.g., Larter et al., 2002; Eagles et al., 2004 and references therein). Exhumation of metamorphic complexes, formation of sedimentary basins and rift-related magmatism (e.g. extensive diking) at ~110–105 Ma were the first responses to separation of Zealandia from West Antarctica (Weaver et al., 1994; Storey et al., 1999) — the final phase of Gondwana breakup. Many models have been proposed to explain the rifting of Zealandia from West Antarctica (Weaver et al., 1994; Storey, 1995, Storey et al., 1999; Mortimer, 2004; Mortimer et al., 2006; Finn et al., 2005; Davy and Wood, 1994; Davy et al., 2008). Several authors have proposed that a plume beneath Marie Byrd Land during the Late Cretaceous caused the break-up of Zealandia from Gondwana (Weaver et al., 1994; Storey, 1995, Storey et al., 1999), whereas others (e.g. Waight et al. 1998a,b) related the inception of intraplate volcanism to lithospheric thinning. Alternative models attributed the change from subduction-related to intraplate volcanism to the collision of the Hikurangi Plateau or Large Igneous Province (LIP) (Fig. 1) with Gondwanaland at what is now the northern margin of the Chatham Rise. The Hikurangi collision caused the subduction zone to be clogged and subduction to shut down (Davy and Wood, 1994; Mortimer et al., 2006; Davy et al., 2008). Luyendyk (1995), on the other hand, proposed the capture of the subducting slab at the northern margin of the Chatham Rise, which was believed to be too young and buoyant to subduct. Slab detachment resulted in the formation of a slab window by 97 Ma (Davy and Wood, 1994; Finn et al., 2005; Mortimer et al., 2006; Davy et al., 2008), which allowed hot, deeper mantle, some possibly related to a starting plume head (Weaver et al. 1994; Storey et al. 1999), to upwell directly beneath the former Gondwana margin, leading to widespread intra-continental rifting and thinning prior to ocean crust formation between Zealandia and West Antarctica at 84 Ma (Larter et al., 2002; Mortimer et al., 2006; Eagles et al., 2004).

Since 84 Ma, Zealandia has drifted north away from Antarctica. Since Antarctica has basically remained stationary in a hotspot reference frame, Zealandia's continental lithosphere has also moved north thousands of kilometers relative to the Earth's sublithospheric mantle. At ~45 Ma, a Pacific–Australia plate boundary propagated through Zealandia (Sutherland, 1995). Initially this boundary was extensional and later strike–slip, causing relative motion between northern and southern parts of Zealandia. Since at least 6 Ma, the Pacific and Australian plates have converged within and near Zealandia, resulting in the uplift of the Southern Alps with subduction zones to the north and south of New Zealand verging to the west and east respectively.

Intraplate igneous activity in Zealandia commenced in the Late Cretaceous (~100 Ma ago). Plutonic and volcanic centers characteristically involved small volumes of magma, forming the Tapuaenuku and Mandamus Igneous Complexes on the South Island of New Zealand (Baker et al., 1994; Tappenden, 2003), and a variety of volcanic centers on and around the eastern Chatham Rise, as well as on the Chatham Islands (Grindley et al., 1977; Panter et al., 2006; Mortimer et al., 2006).

The major Cenozoic intraplate volcanic centers are located on the South Island (Coombs et al., 1986; Weaver and Smith, 1989; Hoernle et al., 2006; Panter et al., 2006; Sprung et al., 2007; Timm et al., 2009) and on the Campbell Plateau (i.e. Campbell, Auckland and Antipodes Islands; Adams, 1983; Gamble et al., 1986; Weaver and Smith, 1989). On the North Island, volumetrically minor Pleistocene intraplate volcanism in the Auckland and Northland areas has been attributed to melting of lithosphere overprinted by Mesozoic or earlier subduction and plume-related magmatism (Huang et al., 1997; Cook et al., 2004).

Please cite this article as: Timm, C., et al., Temporal and geochemical evolution of the Cenozoic intraplate volcanism of Zealandia, Earth-Science Reviews (2009), doi:10.1016/j.earscirev.2009.10.002

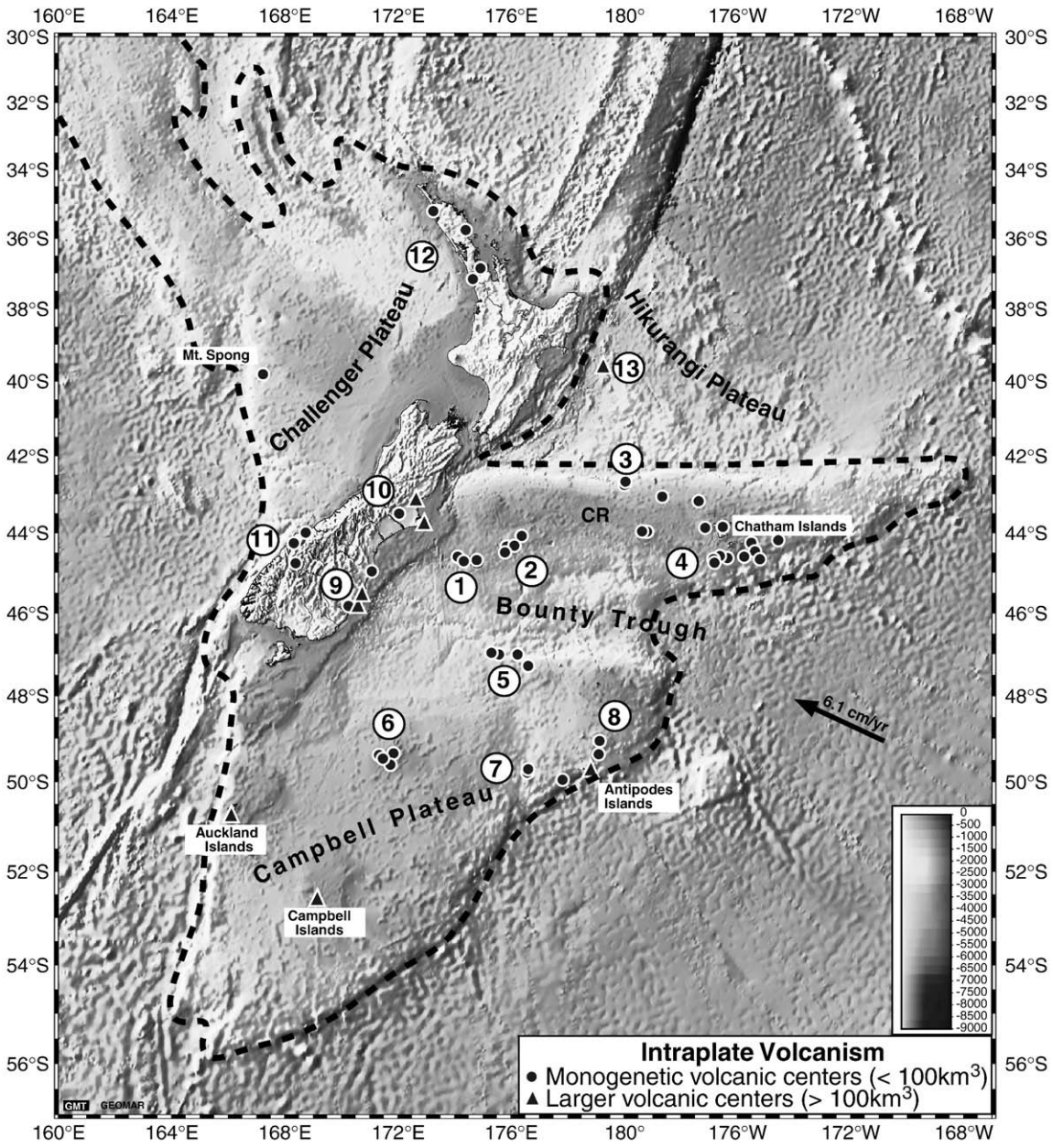

Fig. 1. Bathymetric map of the mainly submerged continent of Zealandia, outlined by the dashed line, and adjacent areas. Sampling sites are shown by black dots marking Cenozoic volcanic centers (monogenetic volcanic fields = circles and larger volcanic complexes/fields with ≥100 km^3, including composite shield volcanoes = triangles). Sampling sites are (1) Urry Knolls, (2) Veryan Bank, (3) Graveyard seamounts, (4) western Chatham Rise, (5) northern Campbell Plateau margin, (6) Pukaki Bank, (7, 8) areas north and west of the Antipodes Islands, (9) Otago volcanic fields (including Timaru/Geraldine) and Dunedin Volcano, (10) Canterbury volcanic fields and Banks Peninsula, (11) Westland, (12) Auckland and Northland volcanic fields, and (13) Rowling B seamount on the Hikurangi Plateau. Plate motion vector is from Clouard and Bonneville (2005).

Submarine intraplate volcanoes have been described from the southern flank of the Chatham Rise (Urry Knolls) (Herzer et al., 1989), from Mt. Spong on the Challenger Plateau (Carey et al., 1991) and from the South Fiji Basin north of the North Island of New Zealand (Mortimer et al., 2007). Geophysical and bathymetric data suggest that intraplate volcanism is common and widespread on submarine portions of Zealandia, which was confirmed during R/V Sonne SO168 and 169 Expeditions (Hoernle et al., 2003; Gohl et al., 2003; Hoernle et al., 2004).

Except for the Dunedin area, the heat flow on the continental plateau of Zealandia is ~60 mW/m^{-2} similar to the averaged global heat flow (~57 mW/m^{-2}) (Sclater et al., 1980; Godfrey et al., 2001). In the Dunedin area, the heat flow is elevated (>90 mW/m^2) (Godfrey et al., 2001) and is accompanied by the highest proportion of mantle helium (~84%) (Hoke et al., 2000) measured in the South Island, suggesting recent magmatic activity in this area. Northward towards Banks Peninsula the heat flow steadily decreases to 'normal' values for continental crust (Godfrey et al., 2001). Based on seismic imaging, the lithospheric thickness beneath Zealandia is generally between 70 and 100 km (Molnar et al., 1999; Stern et al., 2002; Liu and Bird, 2006), but an orogenic root extends up to ~140 km beneath the Southern Alps (Stern et al., 2002).

3. Evolution of Cenozoic magmatism and sample background

Since Early Cretaceous subduction ceased off Zealandia, intraplate volcanism has been widespread on the continent (e.g. Figs. 2 and 3) (Gamble et al., 1986; Weaver and Smith, 1989). Products of this volcanism are primarily mafic, ranging from quartz tholeiite to alkali basalt through trachyte/rhyolite to basanite through phonolite to

Please cite this article as: Timm, C., et al., Temporal and geochemical evolution of the Cenozoic intraplate volcanism of Zealandia, Earth-Science Reviews (2009), doi:10.1016/j.earscirev.2009.10.002

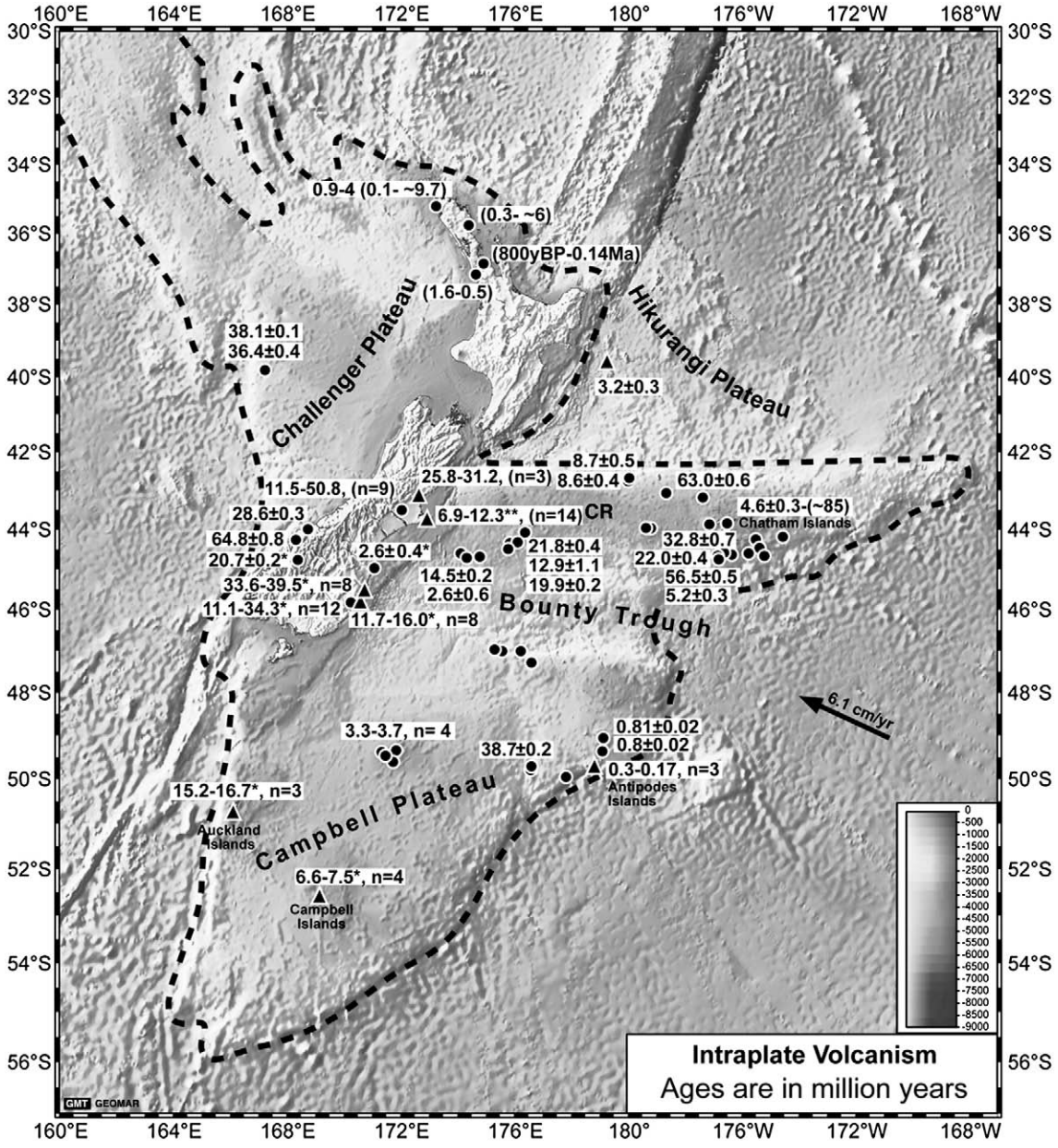

Fig. 2. Ages of intraplate volcanic centers of Zealandia. The Cenozoic volcanoes (black numbers) are irregularly scattered on the Central and Western Chatham Rise, the Campbell and Challenger Plateaus and the South and North Islands of New Zealand, showing no clear age progressions (symbols as in Fig. 1). Age data from Hoernle et al. (2006) are marked with an asterisk, two asterisks refer to age data from Timm et al. (2009) and ages in brackets are taken from Cook et al. (2004) and Smith et al. (1993).

nephelinite and carbonatite. Major episodes of volcanism occurred in the Late Cretaceous, Paleocene to Early Eocene, Late Eocene to Early Oligocene and Middle to Late Miocene (Figs. 4 and 9). Minor activity has been recorded in the Late Oligocene to Early Miocene and Pliocene to Quaternary. The most voluminous volcanism is associated with the Miocene Lyttelton and Akaroa basaltic shield volcanoes (~1600 km^3) on Banks Peninsula and the Dunedin Volcano (~600 km^3) on the Otago Peninsula.

3.1. Northern South Island

The oldest intraplate volcanic rocks in the northern South Island include the mid-Cretaceous alkaline intrusive Tapuaenuku Complex and its associated mid-Cretaceous to Paleocene (100–60 Ma) basanitic to trachybasaltic radial dike swarm (Grapes et al., 1992; Baker et al., 1994) and the mid-Cretaceous alkaline Mandamus Igneous Complex (88–97 Ma) in Canterbury (Tappenden, 2003). The Paleocene to Lower Eocene tholeiitic basalts to basaltic andesites of the View Hill area in Central Canterbury produced K/Ar ages of 51.7 ± 2.4 (all errors are reported at the 2-sigma confidence level) and 47.9 ± 3.6 Ma (Sewell and Gibson, 1988), whereas the tholeiitic to alkaline Cookson Volcanics (≥100 km^3) (McLennan and Weaver, 1984; Morris, 1987) were erupted in the Oligocene. Based on our field studies, the stratigraphically oldest eastern Cookson units are pillow basalts and sheet flows, indicative of submarine volcanic activity, whereas the western Cookson units are characterized by stratigraphically younger conglomerates with large, well-rounded beach cobbles and heavily-oxidized lava flows with top and/or bottom breccias, indicating shallow water to subaerial conditions of emplacement. Therefore we interpret the Cookson Volcanics to have been part of an Oligocene shield volcano, which rose above sea level and formed an island. Based on K/Ar dating, the Oxford volcanics in central Canterbury range in age from 27.1 ± 0.8 to 15.6 ± 1.0 Ma (Sewell and Gibson, 1988). Middle to Late Miocene alkaline to tholeiitic volcanic activity was widespread and produced the large Lyttelton (~350 km^3)

Please cite this article as: Timm, C., et al., Temporal and geochemical evolution of the Cenozoic intraplate volcanism of Zealandia, Earth-Science Reviews (2009), doi:10.1016/j.earscirev.2009.10.002

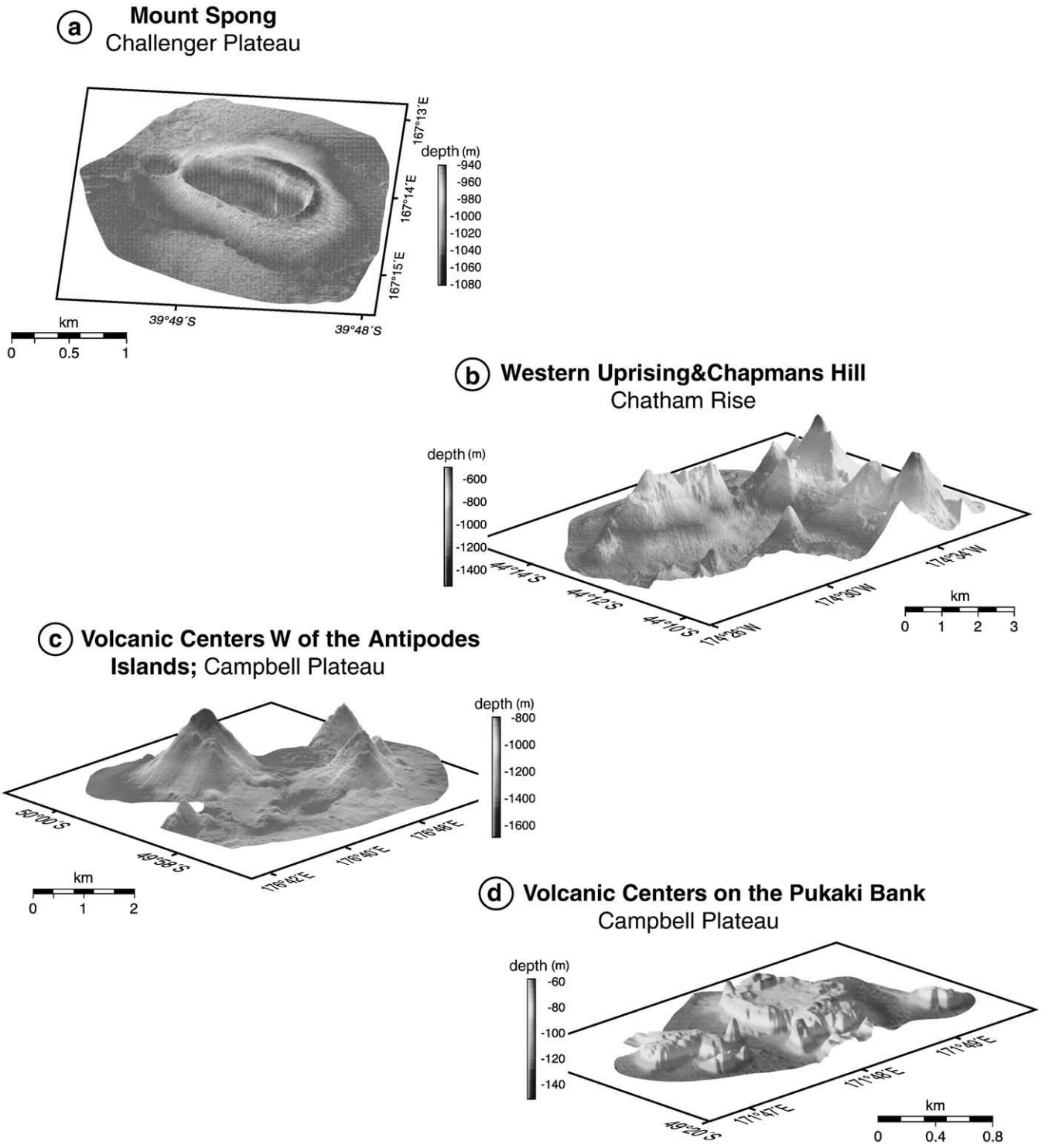

Fig. 3. Oblique views, derived from multibeam bathymetry, showing representative types of submarine volcanism on Zealandia: (a) Mount Spong on the Challenger Plateau, showing two volcanic structures with deep calderas; densely-clustered volcanic ridges and cones (b) of the Western Uprising & Chapmans Hill volcanic field on the Western Chatham Rise and (c) west of the Antipodes Islands (b and c represent the dominant volcanic features on the central and western Chatham Rise and the Campbell Plateau, respectively), and (d) the flat-topped Pukaki Bank with small Holocene cones on the Campbell Plateau.

and Akaroa (~1200 km^3) composite shield volcanoes on Banks Peninsula (Stipp and McDougall, 1968; Weaver and Smith, 1989; Timm et al., 2009). A temporal migration of volcanism on Banks Peninsula from >12 to ~7 Ma towards the southeast corresponds with a compositional evolution to more mafic and Si-undersaturated compositions (from andesites through rhyolites to alkali basalts through trachytes and phonolites to alkali basalts through nephelinites; Timm et al., 2009). Pliocene volcanism on the northern part of the South Island only produced very low-volume transitional basaltic and olivine and quartz tholeiitic lava flows near Geraldine and Timaru (1.3 km^3)

Please cite this article as: Timm, C., et al., Temporal and geochemical evolution of the Cenozoic intraplate volcanism of Zealandia, Earth-Science Reviews (2009), doi:10.1016/j.earscirev.2009.10.002

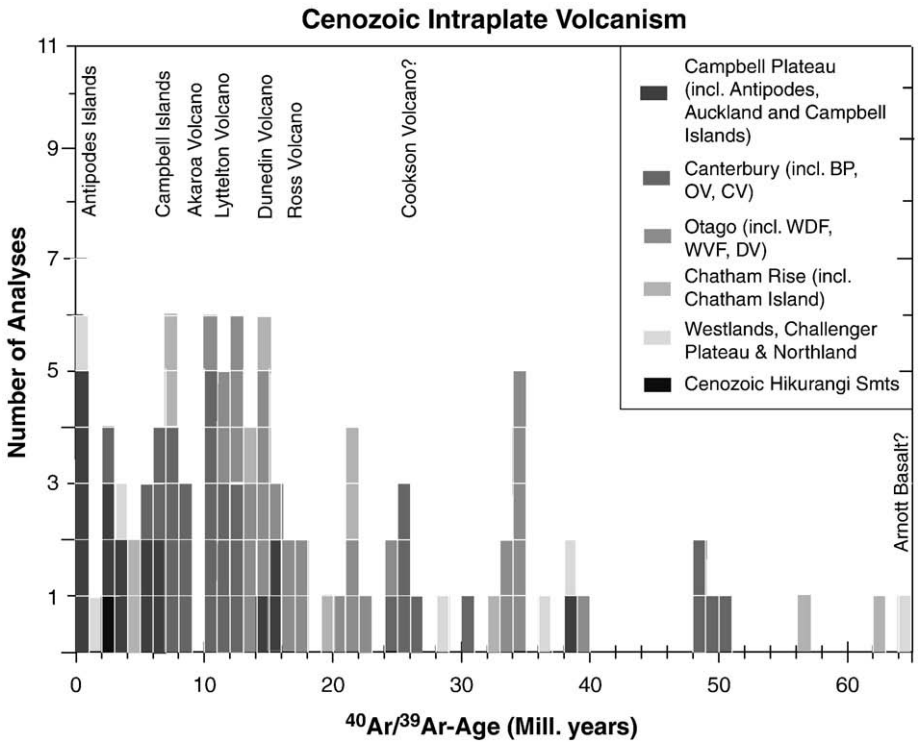

Fig. 4. Histogram showing a complete compilation of our $^{40}Ar/^{39}Ar$ database (including data from Hoernle et al., 2006 and Timm et al., 2009). Although the number of analyses at least in part is likely to reflect a sampling bias with younger volcanism being less likely to be eroded or covered with sediments, there does appear to be an increase with time in the abundance of large magmatic events (≥ 100 km^3), such as composite shield volcanoes (denoted by the vertical text at the time the event primarily took place or the shield volcano was formed).

(Duggan and Reay, 1986) with an $^{40}Ar/^{39}Ar$ age of 2.6 ± 0.4 Ma (Hoernle et al., 2006), which agrees well with a previously determined K/Ar age of 2.5 ± 0.7 Ma (Mathews and Curtis, 1966).

3.2. Southern South Island

The oldest-known volcanic rocks in the Otago region are an ~1 km sequence of Paleocene tuffs drilled offshore of Oamaru (Coombs et al., 1986). The Upper Eocene to Lower Oligocene (40–34 Ma) (Hoernle et al., 2006) Waiareka–Deborah volcanics were largely erupted under submarine conditions (e.g. pillow lavas in Oamaru). Tholeiitic basalts prevail, but rare alkaline volcanism also occurred (Coombs et al., 1986). The basanitic Kakanui Mineral Breccia, with $^{40}Ar/^{39}Ar$ ages of 33.7 ± 0.3 and 34.1 ± 0.1 on amphibole, is the youngest unit of the Waiareka–Deborah group (Hoernle et al., 2006). The Waipiata Volcanics (25–11 Ma) of eastern and central Otago include alkali basalt through mugearite, basanite, nephelinite and phonolite (Coombs et al., 1986; Hoernle et al., 2006; Coombs et al., 2008). The Dunedin shield volcano lies within the Waipiata Volcanic Field. Its lavas range in composition from alkali basalt and basanite to trachyte and phonolite respectively. The dominance of alkali basalt, in contrast to primarily basanite of the Waipiata Volcanics, is consistent with generally higher degrees of melting at overall shallower depths to form the volumetrically larger Dunedin Volcano, which was active for ~4 million years between ~16.0 and ~11.7 Ma (Price and Compston, 1973; McDougall and Coombs, 1973; Hoernle et al., 2006; Coombs et al., 2008).

3.3. Western South Island

Two episodes of mafic mildly alkaline volcanism have been recognized along the west coast of the South Island in South Westland (Sewell and Nathan, 1987). The Late Cretaceous to Paleocene Arnott Basalt was erupted close to the axis of rifting during the separation of New Zealand and Australia (Weaver and Smith, 1989). The Otitia Basalt was erupted during a period of late Eocene crustal extension (Nathan et al., 1986). Both basalts have intraplate affinities. Although the onshore outcrops of these volcanic episodes are limited, geophysical data from magnetic surveys north of the onshore outcrops and offshore seismic profiles suggests that these volcanic episodes were much more extensive (Weaver and Smith, 1989). The Arnott Basalt may have been part of a largely submarine shield volcano. An U/Pb zircon age of 61.4 Ma was obtained from a rhyolitic clast at Porphyry Point, from a deposit that stratigraphically overlies the Arnott Basalt (Phillips et al., 2005), providing a minimum age for the basaltic rocks. The lamprophyric Alpine Dike Swarm extends 110 km southeast from the Alpine Fault. It ranges from nephelinite, basanite and carbonatite to phonolite and trachyte in composition (Cooper, 1986). Cooper et al. (1987) and Cooper and Paterson (2008) proposed that these dikes intruded into tension fractures and Riedel shears at the initiation of the Alpine dextral wrench fault system. K/Ar whole-rock ages from the Alpine Dike Swarm suggest an unusually large age range of 14–846 Ma (Adams, 1980). K/Ar kaersutite ages indicate a much more restricted range of 23–52 Ma (Adams and Cooper, 1996). Rb–Sr and U–Pb dating produced an age range of 20–25 Ma (Cooper et al., 1987). More recent dating of a dike sample on the southeastern edge of the field produced an $^{40}Ar/^{39}Ar$ age of 20.7 ± 0.2 Ma (Hoernle et al., 2006), at the young end of the age ranges determined by other methods.

3.4. Subantarctic islands

Late Cretaceous to Pleistocene volcanic rocks with intraplate geochemical characteristics are present on four Subantarctic island groups. Igneous activity on the Chatham Islands can be divided in three phases: Late Cretaceous (85–82 Ma; Southern Volcanics), Eocene–Oligocene (41–35 Ma; Northern Volcanics) and Miocene–Pliocene (~5 Ma; Rangitihi Volcanics) (Panter et al., 2006). With

Please cite this article as: Timm, C., et al., Temporal and geochemical evolution of the Cenozoic intraplate volcanism of Zealandia, Earth-Science Reviews (2009), doi:10.1016/j.earscirev.2009.10.002

decreasing age, the volcanic rocks became progressively more Si-undersaturated, from ol-rich basalt to basanite. More-voluminous volcanism is associated with the Ross and Carnley Volcanoes of the Auckland Islands. $^{40}Ar/^{39}Ar$ ages of 15.2 ± 0.2 Ma and 16.7 ± 0.6 were determined for the Ross Volcano (Hoernle et al., 2006), indicating that it was active at a similar time as the Dunedin Volcano (c. 12–16 Ma) (Hoernle et al., 2006). There is some question about the large K/Ar age ranges of 12–25 Ma for the Ross Volcano and 17–37 Ma for the Carnley Volcano (Adams, 1983). Based on detailed age dating of the younger Banks and Dunedin volcanoes, which are also much better exposed and accessible, we see that these volcanoes generally have a peak in activity over 1–2 million years and then low levels of activity for the next 3–5 million years (Hoernle et al., 2006; Timm et al., 2009). If the Ross and Carnley shield volcanoes were formed by similar processes to the shield volcanoes on the South Island, we would expect age ranges for these volcanoes on the order of 4–6 Ma and therefore suspect that some of the K/Ar ages are inaccurate due to alteration of the samples. Two lavas from Campbell Island give $^{40}Ar/^{39}Ar$ ages of 7.5 ± 0.1 to 6.6 ± 0.3 Ma (Hoernle et al., 2006), falling into the K/Ar age range of 6.5–8.5 (Adams et al., 1979). The Antipodes Islands, located on the northeastern edge of the Campbell Plateau consist of silica-undersaturated (basanite to nepheline hawaiite to phonolite) volcanic rocks (Gamble et al., 1986). Two K/Ar dates of 0.25 and 0.50 Ma suggest that this volcano may have formed in the Pleistocene (Cullen, l969). On the North Island of New Zealand intraplate volcanism was active between ~11 Ma and ~600 yrs ago in the Northland area (Smith et al., 1993), whereas volcanic activity in the South Auckland Volcanic Field took place between ~2 Ma and 200 yrs ago (Briggs et al., 1994) and thus include the youngest intraplate volcanic rocks known on Zealandia.

The common occurrence of pillow lavas and sheet flows, partly with glassy margins, on the South Island of New Zealand (e.g. within the Waiareka Deborah Formation at Oamaru, the View Hill Basalts, etc.) implies that Zealandia was, through most of the Cenozoic, submerged (e.g. Landis et al., 2008). Only a few volcanic centers emerged above sea level, such as the Cookson Volcanic Complex, and the Dunedin and Banks Peninsula volcanoes, which began erupting under submarine conditions (e.g. Weaver and Smith, 1989).

3.5. Other offshore regions

Submarine intraplate volcanoes have been described from the southern flank of Chatham Rise (Urry Knolls) (Herzer et al., 1989), from Mt. Spong on the Challenger Plateau and from the South Fiji Basin north of the North Island of New Zealand (Mortimer et al., 2007). Geophysical and bathymetric data suggested that intraplate volcanoes were common and widespread on submarine portions of Zealandia, and this was confirmed during R/V Sonne expeditions SO168 and 169 (Hoernle et al., 2003, 2004, Gohl et al., 2003).

On the SO168 and 169 expeditions, more than 40 volcanic structures were mapped on or near the Chatham Rise and on the Campbell and Challenger Plateaus using a SIMRAD EM120 multi-beam echo-sounding system. The volcanoes on the central and western Chatham Rise and on the Campbell Plateau rarely exceed 1–3 km in basal diameter and some hundreds of meters in height. Their bases are located at water depths of ~1500 m–60 m. The volcanism in these regions primarily occurs in localized areas, such as around the Chatham Islands, the Graveyard Seamount area, the Veryan Bank area and at the Urry Knolls on the Chatham Rise and the Pukaki Bank, north and west of the Antipodes Island and the northern margin of the Campbell Plateau (Fig. 1). Each of the submarine Cenozoic volcanic centers has a distinct morphology. Mount Spong on the Challenger Plateau, for instance, only rises ~100 m above the surrounding ocean floor, but contains two WNW–ESE aligned oval-shaped calderas (overall ~2 × 0.8 km), the floors of which lie at greater depths than the surrounding seafloor (Fig. 3a). Probably this structure was higher than 100 m in the past, but has been almost entirely buried by Cenozoic sediments. Chapmans Hill and Western Uprising on the Chatham Rise consist, in contrast, of volcanic cones and ridges rising up to 1000 m above their bases to ~500 mbsl (Fig. 3b). North and South of the Antipodes Islands on the Campbell Plateau numerous small volcanic cones were mapped, which show comparable morphologies to those on the Chatham Rise, reaching maximum heights of about 600 m above the seafloor, with basal diameters of ~2 km at ~1400 mbsl (Fig. 3c). In the central part of the Campbell Plateau, several volcanic structures, with bases ~1 km in diameter and flat tops at ~60 mbsl, are located on the Pukaki Bank. The flat tops of the Pukaki Bank volcanoes may also represent post-eruptive erosional platforms. Voluminous Cenozoic volcanic structures appear to be restricted to the Chatham, Campbell, Auckland, and Antipodes Islands (and possibly the Pukaki Bank). The morphology of the submarine volcanic features overall is comparable to that of volcanic centers on the South Island of New Zealand. There are two volcanic end members — widely distributed monogenetic volcanic fields, and large composite shield volcanoes (e.g. Hoernle et al., 2006), which are shown by different symbols in Fig. 1.

3.6. Sampling and analytical methods

For the present study, volcanic rocks were dredged from 26 now submerged volcanoes on the central and western Chatham Rise, 13 locations on the Campbell Plateau, 2 locations from Mount Spong on the Challenger Plateau and 1 location on the Hikurangi Plateau (Fig. 1). At all dredge sites discussed here, the angular shape of the rocks, freshly broken surfaces, and the homogeneity of rock types indicate an in-situ (not ice-rafted) origin for the dredged rocks. Subaerial volcanic areas of New Zealand were sampled during three field seasons. Sampling localities are summarized in Supplementary File 1.

Analyses of $^{40}Ar/^{39}Ar$ were conducted on matrix chips and biotite and feldspar phenocrysts at the IFM-GEOMAR Tephrochronology Laboratory. The particles were hand-picked under a microscope from crushed and sieved splits. All separates were cleaned using an ultrasonic disintegrator. Plagioclase phenocrysts were additionally etched in 5% hydrofluoric acid for 15 minutes. Samples were neutron irradiated at the 5-MW reactor of the GKSS Research Center (Geesthacht, Federal Republic of Germany), with crystals and matrix chips in aluminum trays and irradiation cans wrapped in 0.7 mm cadmium foil. Laser $^{40}Ar/^{39}Ar$ age determinations were performed on single crystals of feldspar phenocrysts, that were fused individually, and on matrix chips, that were analyzed by laser step-heating analysis. Purified gas samples were analyzed using a MAP 216 series noble gas mass spectrometer. Raw mass spectrometer peaks were corrected for mass discrimination, background and blank values determined every fifth analysis. The neutron flux was monitored using Taylor Creek Rhyolite Sanidine (TCR-2: 27.87 ± 0.04 Ma) (Lanphere, unpubl. data). Vertical variations in *J*-values were quantified by a cosine function fit. Corrections for interfering neutron reactions on Ca and K are based on analyses of optical grade CaF_2 and high-purity K_2SO_4 salt crystals that were irradiated together with the samples. Replicate analyses of 8–13 particles from each phase were carried out for statistical reasons in order to calculate mean apparent ages and isochron ages. Internal errors are reported at the 2-sigma confidence level.

Samples selected for geochemistry were first crushed to small pieces, then washed in deionized water and carefully hand-picked under a binocular microscope. Major elements and some trace elements (e.g., Cr, Ni, Zr, Sr) of whole-rock samples were determined on fused beads using a Philips X'Unique PW1480 X-ray fluorescence spectrometer (XRF) equipped with a Rh-tube at IFM-GEOMAR. H_2O and CO_2 were analyzed in an infrared photometer (Rosemount CSA 5003). Additional trace elements (e.g., Rb, Ba, Y, Nb, Ta, Hf, U, Th, Pb

Please cite this article as: Timm, C., et al., Temporal and geochemical evolution of the Cenozoic intraplate volcanism of Zealandia, Earth-Science Reviews (2009), doi:10.1016/j.earscirev.2009.10.002

Table 1
Results of step-heating and single-crystal $^{40}Ar/^{39}Ar$ analyses.

Sample ID	Group	Mean apparent age or plateau age (Ma)	2σ	MSWD	%^{39}Ar in plateau	*n*	Dated Material and type of analyses
Western and Central Chatham Rise							
SO168-DR91-1	lsg	63.04	±0.61	1.30	83.2		Matrix step heat
SO168-DR87-6	hsg EMII	56.53	±0.47	1.1	70.4		Matrix step heat
SO168-DR74-1	lsg	32.76	±0.65	0.53	92.3		Matrix step heat
SO168-DR80-1	lsg	22.04	±0.38	1.60	71.1		Matrix step heat
SO168-DR97-1	lsg	21.78	±0.38	1.60	69.8		Matrix step heat
SO168-DR99-2	lsg	19.87	±0.24	1.18	84.8		Matrix step heat
SO168-DR101-1	lsg	14.45	±0.22	0.68	100.0		Matrix step heat
SO168-DR96-1	lsg	12.90	±1.10	2.3	62.4		Matrix step heat
SO168-DR3-1	lsg	8.70	±0.45	1.5	71.5		Matrix step heat
SO168-DR5-1	lsg	8.60	±0.43	1.4	88.2		Matrix step heat
SO168-DR87-4	hsg EMII	5.16	±0.27	1.5	81.5		Matrix step heat
Rowling B Seamount on Hikurangi Plateau							
SO168-19-1	lsg	3.32	±0.27	0.47	82.0		Matrix step heat
Chatham Islands							
P74894	lsg	4.62	±0.28	1.40	86.8		Matrix step heat
Challenger Plateau							
SO168-DR2-1	lsg	38.05	±0.10	1.90		12	Fsp single-crystal
SO168-DR2-2	lsg	36.41	±0.09	1.00		13	Fsp single-crystal
Campbell Plateau							
SO169-DR6-1	lsg	38.71	±0.20	1.30	56.7		Matrix step heat
SO169-DR11-5	lsg	3.66	±0.25	0.77	55.8		Matrix step heat
SO169-DR15-1	lsg	3.63	±0.17	1.16	99.8		Matrix step heat
SO169-DR12-1	lsg	3.39	±0.22	1.6	86.6		Matrix step heat
SO169-DR11-1	lsg	3.34	±0.19	1.30	98.2		Matrix step heat
SO169-DR3-7	lsg	0.81	±0.03	1.08		18	Fsp single-crystal
SO169-DR3-1	lsg	0.80	±0.03	1.11		18	Fsp single-crystal
A109	lsg	0.30	±0.11	0.88	99.9		Matrix step heat
A8B	lsg	0.18	±0.06	0.58	89.8		Matrix step heat
A105	lsg	0.17	±0.18	0.72	99.2		Matrix step heat
Canterbury: Cookson Volcanics							
MSI36 A	lsg	31.18	±0.59	1.60	69.4		Matrix step heat
MSIK33 A	lsg	26.60	±0.28	0.86	72.8		Matrix step heat
MSI42 C	lsg	25.82	±0.54	0.80	57.5		Matrix step heat
Canterbury: Oxford Volcanics							
MSI180 B	hsg EMII	50.77	±0.50	0.72	73.0		Matrix step heat
MSI24	hsg EMII	50.00	±1.10	0.63	75.3		Fsp step heat
MSI23 A	hsg EMII	49.30	±1.10	0.57	80.1		Fsp step heat
MSI25	Hsg EMII	48.80	±2.10	2.00	59.3		
MSI27 A	hsg EMII	25.61	±0.58	1.60	58.6		Matrix step heat
MSI22 B	hsg EMII	25.20	±0.12	1.13	86.8		Fsp step heat
MSI22 B	hsg EMII	25.55	±0.21	0.37	53.0		Biot step heat
MSI181	hsg EMII	12.20	±1.00	0.93	95.5		Matrix step heat
MSI21 A	hsg EMII	11.49	±0.75	2.40	76.2		Fsp step heat
Westland: Otitia and Arnott Basalts							
MSI65 A	lsg	64.80	±0.81	1.16	60.1		Fsp step heat
MSI63 A	lsg	28.55	±0.31	2.1	71.1		Matrix step heat
Otago: Dunedin Volcano and Waipiata Volcanic Field							
FouldenV2A	lsg	23.17	±0.37	1.40	92.8		Matrix step heat
MSI88 A	lsg	14.57	±0.33	0.77	49.3		Fsp step heat
OU22636	lsg	11.66	±0.08	1.40	87.0		Fsp step heat
Northland							
NZN3	hsg MORB	4.00	1.4	0.73	68.8		Fsp step heat
NZN28	hsg MORB	1.97	0.68	1.60	98.1		Fsp step heat
NZN32	hsg MORB	0.88	0.53	1.14	100		Fsp step heat

Abbr.: lsg = low-silica group; hsg = high-silica group.
Detailed information is supplied as Supplementary Files 2 and 3.

and all REE) were determined by ICP-MS on a VG Plasmaquad PQ1-ICP-MS at the Institute of Geosciences (University of Kiel) after the methods of Garbe-Schönberg (1993).

Sr–Nd isotope analyses of the submarine samples were carried out on rock powders, leached in 6 N HCl at 130 °C for up to 24 hours prior to dissolution in a 5:1 mixture of concentrated ultra-pure (u.p.) HF

Please cite this article as: Timm, C., et al., Temporal and geochemical evolution of the Cenozoic intraplate volcanism of Zealandia, Earth-Science Reviews (2009), doi:10.1016/j.earscirev.2009.10.002

and HNO3. Hf and Pb isotope analyses were carried out on unleached powders and rock chips respectively. The element chromatography followed the methods outlined in Hoernle et al. (1991) and Hoernle et al. (2008). Sr–Nd–Pb isotopic ratios were determined on the TRITON and MAT262 RPQ^{2+} thermal ionization mass spectrometers (TIMS) at IFM-GEOMAR with both instruments operating in static multi-collection mode. Sr and Nd isotopic ratios were normalized within run to $^{86}Sr/^{88}Sr = 0.1194$ and $^{146}Nd/^{144}Nd = 0.7219$, respectively. All Sr isotope data are reported relative to NBS987 $^{87}Sr/^{86}Sr = 0.710250$ with an external $2\sigma = 0.000012$ ($N = 32$) for the MAT262 and $2\sigma = 0.000009$ ($N = 26$) for the TRITON. The Nd isotope data, generated on the TRITON, are reported relative to La Jolla $^{143}Nd/^{144}Nd = 0.511849 \pm 0.00007$ ($N = 33$) and to an in-house monitor Spex $^{143}Nd/^{144}Nd = 0.511715 \pm 0.00007$ ($N = 26$). The long-term NBS 981 ($N = 125$) values are $^{206}Pb/^{204}Pb = 16.898 \pm 0.006$, $^{207}Pb/^{204}Pb = 15.437 \pm 0.007$, $^{208}Pb/^{204}Pb = 36.527 \pm 0.024$ and corrected to the NBS 981 values given in Todt et al. (1996). Total chemistry blanks were <400 pg for Sr, Nd, Hf and Pb and thus considered negligible. Hafnium was separated following a two-column procedure as described by Geldmacher et al. (2003). Hafnium isotope ratios were carried out on a VG Axiom multi-collector ICPMS (MC-ICPMS). After two days of measuring the in-house spex monitor to stabilize the signal, standards was determined repeatedly every two or three samples to verify the machine performance. To correct the instrumental mass bias $^{176}Hf/^{177}Hf$ was normalized to $^{179}Hf/^{177}Hf = 0.7325$.

4. Results

4.1. $^{40}Ar/^{39}Ar$ dating

Our 45 new $^{40}Ar/^{39}Ar$ ages from Cenozoic volcanic rocks across Zealandia range from 64.8 ± 0.4 to 0.17 ± 0.09 Ma (Figs. 2 and 4). A summary list of all $^{40}Ar/^{39}Ar$ age data can be found in Table 1. All errors are stated at the 2σ confidence level (see Supplementary Files 1 and 2 for more details).

Only a few samples yielded early Cenozoic $^{40}Ar/^{39}Ar$ ages between ~65 and 40 Ma. On the South Island of New Zealand, a sample of the Arnott Basalt was dated at 64.8 ± 0.4 Ma by $^{40}Ar/^{39}Ar$ step heating of feldspar (fsp), consistent with the U–Pb zircon age of 61.4 ± 0.8 Ma obtained from a rhyolitic clast in a deposit that stratigraphically overlies the Arnott Basalt (Phillips et al., 2005). Since the Arnott Basalt is on the Australian Plate, the Arnott Basalt must have been located close to the Auckland Islands when these rocks were erupted (e.g. Sutherland, 1995). The oldest Cenozoic ages for offshore volcanism are from a volcanic cone on the central Chatham Rise ($^{40}Ar/^{39}Ar$ age of 63.0 ± 0.6 Ma; matrix step heat) and from a seamount south of the Chatham Islands ($^{40}Ar/^{39}Ar$ age of 56.5 ± 0.5 Ma; matrix step heat). Samples from the View Hill Volcanics in central Canterbury yielded a restricted age range with ages of 50.8 ± 0.3, 50.0 ± 1.1, 49.3 ± 0.6 and 48.9 ± 0.7 Ma (fsp and matrix step heating, within the slightly larger K/Ar age range of 48–52 Ma) (Sewell and Gibson, 1988).

Volcanism in the late Eocene and early Oligocene was widespread, occurring at small volcanic centers west of the Antipodes Islands (38.7 ± 0.2 Ma; matrix step) and on the central Chatham Rise (Chapmans Hill; 32.8 ± 0.7 Ma; matrix step heat), at Mount Spong (feldspar single fusion $^{40}Ar/^{39}Ar$ ages of 38.1 ± 0.1 and 36.4 ± 0.09; $n = 12$ and 13, respectively). On land the Cookson Volcanics in southern to central Canterbury on the South Island gave three matrix step heat $^{40}Ar/^{39}Ar$ ages of 31.2 ± 0.6, 26.6 ± 0.3 and 25.8 ± 0.5 Ma, which overlap with the age of the Otitia Basalts in Westland (28.6 ± 0.3 Ma; matrix step heat). We note that our Late Oligocene age is not consistent with the Otitia basalt having formed during a period of Late Eocene extension as previously proposed (Nathan et al., 1986). Since the Otitia Basalts are, like the Arnott Basalt, on the Australian Plate, they were emplaced several hundred kilometers south of most of the South Island, which was located on the Pacific Plate.

Late Oligocene and Miocene volcanism was widespread on Zealandia. Two alkali basalts in central Canterbury collected along the Eyre River (Oxford area) yielded late Oligocene $^{40}Ar/^{39}Ar$ ages of 25.6 ± 0.6 (matrix step heat) and 25.6 ± 0.2 Ma (biotite age; slightly lower feldspar age of 25.2 ± 0.1 Ma for the same sample). The $^{40}Ar/^{39}Ar$ ages fall at the older end of the K/Ar age range of 30–11 Ma, determined for the Oxford volcanics (McLennan and Weaver, 1984; Sewell and Gibson, 1988). Early to mid Miocene volcanic activity took place on the Central Chatham Rise, near the Chatham Islands (Charlton A Seamount, 22.0 ± 0.4 Ma; matrix step heat), western Chatham Rise (Orton/Vernon Bank, Anja Seamount and Veryan Bank, 21.8 ± 0.4, 19.9 ± 0.2 and 12.9 ± 1.1 Ma, respectively, matrix step heat ages) and at the Urry Knolls (Jordan Seamount; 14.5 ± 0.2 Ma; matrix step heat). In southern and central Canterbury (Oxford area) two mid Miocene ages of 12.2 ± 1.0 and 11.5 ± 0.8 Ma (matrix and feldspar step heat, respectively) were determined on lavas of Burnt and Harper Hills and thus fall within the K/Ar range determined by Sewell and Gibson (1988) for the Harper Hill basalt (13.5–11.0 Ma). A sample from the Waipiata Volcanic Field produced a matrix step heat age of 23.2 ± 0.4 Ma, placing it at the earlier end of the Waipiata volcanism, which ranges from 25 to 11 Ma (Hoernle et al., 2006; Coombs et al., 2008). Two additional step heat ages from the Dunedin Volcano of 14.6 ± 0.3 (feldspar) and 11.7 ± 0.1 (feldspar) Ma also fall within the previous range established for the Dunedin Volcano of 16–12 Ma (Hoernle et al., 2006; Coombs et al., 2008). Lavas from the Graveyard Seamounts on the northern central Chatham Rise yielded late Miocene ages of 8.7 ± 0.5 and 8.6 ± 0.4 Ma (both matrix step heat ages).

Pliocene volcanic rocks are widespread on Zealandia. The youngest volcanic succession on the Chatham Islands yielded a $^{40}Ar/^{39}Ar$ (matrix step heat) of 4.6 ± 0.3 Ma. A sample from Perry Seamount on the central Chatham Rise, near the Chatham Islands, produced a matrix step heat age of 5.2 ± 0.3 Ma. Four samples from the Pukaki Bank on the Campbell Plateau yielded ages of 3.7 ± 0.3 Ma, 3.6 ± 0.2, 3.4 ± 0.2 and 3.3 ± 0.2 Ma (matrix step heat ages), identical within error. A Pliocene matrix step heat age of 3.3 ± 0.3 was also determined on a volcanic rock from Rowling B seamount, located on the Hikurangi Plateau. Three additional Pliocene to Quaternary feldspar step heat $^{40}Ar/^{39}Ar$ ages of 4.0 ± 1.4, 2.0 ± 0.7 and 0.88 ± 0.5 Ma were determined on lavas from Northland on the North Island of New Zealand, which fall into the range of existing K/Ar ages of volcanic rocks from the Northland (e.g. Smith et al., 1993).

In the Quaternary several pulses of volcanism formed volcanic cones around the Antipodes Island giving two identical $^{40}Ar/^{39}Ar$ ages within error of 0.81 ± 0.03 and 0.80 ± 0.03 Ma (feldspar single fusion; both $n = 18$). Three matrix step heat ages of 0.3 ± 0.1, 0.18 ± 0.1 and 0.17 ± 0.2 Ma were obtained for onland Antipodes Island lavas, extending the 0.25–0.50 Ma K/Ar age range for the Antipodes reported by Cullen (1969) to even younger ages.

In summary, our new $^{40}Ar/^{39}Ar$ data set reveals that Cenozoic intraplate volcanism was widespread across the submerged part of Zealandia. Our new data also give new and more precise information on the temporal distribution of intraplate volcanism on the emergent islands of Zealandia (Fig. 4). Our new age data generally confirm the published age data for North, South and Subantarctic islands volcanism where available and add new radiometric ages for areas where none existed before (e.g. Cookson Volcanics; Otitia and Arnott Basalts). The existence of only a few ages between 65 and 40 Ma may indicate lower levels of volcanic activity in the early Cenozoic. An overall sampling bias, however, may be present due to older rocks having been eroded or covered with sediment. Although large shield-type volcanoes also formed in the early and mid Cenozoic, ~ 65–25 Ma (e.g. possibly Arnott Basalts including offshore outcrops and Cookson volcanics), shield volcanoes appear to become more abundant in the last 25 Ma (e.g. Dunedin, Auckland Island, Banks Peninsula, Campbell Islands in the Miocene, Pukaki Bank volcanoes in the Pliocene and Antipodes Island in the Quaternary).

Please cite this article as: Timm, C., et al., Temporal and geochemical evolution of the Cenozoic intraplate volcanism of Zealandia, Earth-Science Reviews (2009), doi:10.1016/j.earscirev.2009.10.002

Table 2
Sr–Nd–Pb–Hf isotope data.

Sample number	Location	Group	$^{87}Sr/^{86}Sr$	$^{143}Nd/^{144}Nd$	$^{206}Pb/^{204}Pb$	$^{207}Pb/^{204}Pb$	$^{208}Pb/^{204}Pb$	$^{176}Hf/^{177}Hf$
Western Chatham Rise								
SO168-DR3-1	Graveyard A	lsg	0.703492 (2)	0.512852 (2)	19.499 (8)	15.636 (6)	39.427 (16)	
SO168-DR5-1	Morgue (Graveyards)	lsg	0.703729 (8)	–	19.341 (1)	15.624 (1)	39.134 (2)	
SO168-DR5-4	Morgue (Graveyards)	lsg	0.703441 (3)	0.512832 (2)	19.868 (1)	15.648 (1)	39.659 (2)	
SO168-DR74-2	Chapmans Hill	lsg	0.702710 (5)	0.513030 (3)	19.164 (2)	15.553 (1)	38.628 (3)	
SO168-DR74-4	Chapmans Hill	lsg	0.702713 (3)	0.513042 (3)	19.236 (1)	15.558 (4)	38.762 (14)	
SO168-DR79-1	Howson D	lsg	0.703310 (5)	0.512858 (3)	20.422 (3)	15.680 (2)	40.052 (6)	
SO168-DR80-1	Charlton A	lsg	0.703196 (5)	0.512817 (2)	19.952 (1)	15.657 (1)	39.608 (2)	
SO168-DR80-6	Charlton A	lsg	0.703183 (3)	0.512832 (2)	20.108 (4)	15.668 (14)	39.793 (38)	
SO168-DR81-1	Charlton B	lsg	0.703182 (3)	0.512863 (3)	19.856 (1)	15.645 (0)	39.464 (1)	
SO168-DR83-2	FBI	lsg	0.702809 (2)	0.512990 (12)	18.910 (1)	15.651 (1)	38.791 (1)	
SO168-DR84-2	Gore	lsg	0.703010 (3)	0.512889 (2)	19.540 (1)	15.618 (0)	39.005 (2)	
SO168-DR84-4	Gore	lsg	–	–	19.956 (1)	15.629 (1)	39.649 (2)	
SO168-DR87-1	Perry	hsg EMII	0.703147 (3)	0.512867 (3)	19.301 (4)	15.623 (1)	39.026 (4)	
SO168-DR87-4	Perry	hsg EMII	0.703132 (3)	0.512874 (3)	19.321 (2)	15.630 (1)	39.064 (3)	
SO168-DR87-6	Perry	hsg EMII	0.703111 (2)	0.512871 (4)	19.319 (3)	15.631 (2)	39.047 (6)	
SO168-DR88-1	Thompson	lsg	0.702950 (2)	0.512936 (3)	19.805 (3)	15.599 (5)	39.372 (4)	
SO168-DR89-4	Clerke A	lsg	0.703068 (2)	0.512883 (3)	19.952 (29)	15.636 (23)	39.811 (58)	
SO168-DR91-1	Manley	lsg	0.703806 (3)	0.512889 (3)	19.294 (2)	15.630 (2)	38.953 (4)	
SO168-DR96-1	Silke	hsg EMII	0.703248 (2)	0.512842 (3)	19.402 (4)	15.642 (3)	39.201 (8)	
SO168-DR97-1	Orton	lsg	0.702861 (2)	0.512868 (3)	20.088 (1)	15.649 (1)	39.703 (3)	
SO168-DR98-2	Gathrey	lsg	0.702871 (2)	0.512880 (3)	20.226 (3)	15.658 (2)	39.755 (5)	
SO168-DR99-1	Anja	lsg	0.702933 (3)	0.512901 (4)	20.090 (20)	15.651 (7)	39.674 (7)	
SO168-DR101-1	Jordan	hsg EMII	0.703958 (5)	0.512804 (3)	18.860 (1)	15.606 (1)	38.972 (2)	
SO168-DR104-1	Forwood	lsg	0.703055 (3)	0.512949 (3)	19.814 (1)	15.629 (1)	39.532 (2)	
SO168-DR105-1	Bootie	hsg EMII	0.702996 (3)	0.512932 (2)	19.502 (1)	15.619 (1)	39.251 (2)	
Chatham Islands								
P75894	The Horns	lsg	0.703171 (4)	0.512865 (3)	20.620 (1)	15.680 (1)	40.279 (2)	0.282949 (7)
P74899	Cape L'Evenque	lsg	0.703023 (5)	0.512874 (2)	19.652 (1)	15.639 (1)	39.192 (2)	
Cenozoic Hikurangi Plateau Seamount								
SO168-DR19-1	Rowling B Smt.	lsg	0.703088 (4)	0.512832 (3)	19.644 (0)	15.648 (0)	39.307 (1)	0.282949 (7)
Challenger Plateau								
SO168-DR2-1	Mount Spong	lsg	0.703158 (5)	0.512860 (3)	20.421 (1)	15.664 (1)	40.022 (2)	
SO168-DR2-2	Mount Spong	lsg	0.703200 (3)	0.512867 (3)	20.670 (4)	15.710 (3)	40.653 (7)	
Cambell Plateau								
SO169-DR3-1K	N of Antipodes Is.	lsg	0.703116 (3)	0.512900 (3)	20.306 (1)	15.664 (1)	39.620 (3)	
SO169-DR3-7	N of Antipodes Is.	lsg	0.703102 (5)	0.512903 (3)	20.247 (1)	15.658 (1)	39.580 (3)	
SO169-DR6-1	W of Antipodes Is.	lsg	0.703172 (3)	0.512892 (3)	19.255 (2)	15.567 (1)	38.904 (3)	
SO169-DR11-1	Pukaki Bank	lsg	0.703008 (2)	0.512964 (3)	19.776 (3)	15.604 (3)	39.319 (7)	
SO169-DR11-5	Pukaki Bank	lsg	0.703019 (5)	0.512952 (3)	19.755 (1)	15.589 (1)	39.264 (2)	
SO169-DR12-1	Pukaki Bank	lsg	0.703132 (2)	0.512940 (3)	19.652 (2)	15.597 (1)	39.249 (4)	
SO169-DR15-1	Pukaki Bank	lsg	0.703221 (5)	0.512925 (2)	19.584 (1)	15.595 (1)	39.207 (2)	
A105	Antipodes Islands	lsg	0.702939 (3)	0.512914 (3)	20.507 (3)	15.665 (2)	39.759 (6)	
A109	Antipodes Islands	lsg	0.702904 (2)	0.512917 (2)	20.493 (3)	15.652 (2)	39.730 (5)	
Northland								
NZN3	Cable Bay	hsg MORB	0.702918 (5)	0.513013 (3)	18.910 (1)	15.585 (1)	38.586 (2)	
NZN28	Near Lake Omapeu	hsg MORB	0.703315 (5)	0.512963 (3)	18.810 (1)	15.592 (1)	38.584 (1)	
NZN29	Tuanui Quarry	hsg MORB	0.702767 (4)	0.513014 (3)	19.002 (1)	15.577 (1)	38.592 (2)	
NZN30	NW of Kerikeri	hsg MORB	0.702702 (5)	0.513061 (2)	18.781 (1)	15.544 (1)	38.409 (2)	
NZN31	East side of Kerikeri	hsg MORB	0.703324 (5)	0.513082 (3)	18.625 (2)	15.537 (1)	38.269 (3)	
NZN32	East side of Kerikeri	hsg MORB	0.703281 (20)	0.512962 (3)	18.891 (1)	15.596 (1)	38.623 (2)	
Marlborough: Grasseed Volcanics								
P 50272 B	Grasseed Volcanics	lsg	0.703800 (3)	0.512853 (3)	19.918 (2)	15.668 (1)	39.531 (4)	0.282874 (5)
Canterbury: Oxford Area								
MSI 21A	Harper Hill	hsg EMII	0.703509 (2)	0.512913 (2)	19.460 (1)	15.613 (1)	39.204 (2)	0.283054 (11)
MSI 22B	Acheron Gabbro	hsg EMII	0.703845 (3)	0.512810 (2)	19.003 (1)	15.640 (1)	38.816 (2)	0.282896 (12)
MSI 23A	View Hill	hsg EMII	0.704161 (3)	0.512805 (3)	19.052 (1)	15.629 (1)	38.905 (2)	
MSI 25	View Hill	hsg EMII	0.704169 (2)	0.512794 (3)	18.988 (2)	15.624 (2)	38.843 (4)	
MSI 27A	View Hill	hsg EMII	0.703880 (5)	0.512788 (3)	19.136 (1)	15.648 (1)	38.925 (2)	
MSI 180A	View Hill	hsg EMII	0.704172 (3)	0.512799 (3)	19.047 (2)	15.632 (1)	38.923 (4)	
MSI 181	Burnt Hill	hsg EMII	0.704048 (3)	0.512819 (3)	19.072 (1)	15.632 (1)	38.890 (3)	
Canterbury: Cookson Volcanics								
MSIK 33A	Little Lottery River	lsg	0.703001 (5)	0.512871 (3)	20.175 (3)	15.658 (2)	39.687 (6)	
MSI 36A	Main Lottery River	lsg	0.703084 (3)	0.512840 (3)	19.991 (5)	15.676 (4)	39.647 (10)	
MSI 41B	Waiau River	lsg	0.703301 (5)	0.512814 (3)	20.403 (1)	15.718 (1)	40.092 (2)	
MSI 42C	Mason River	lsg	0.703670 (5)	0.512870 (2)	19.582 (1)	15.634 (1)	39.235 (3)	0.282910 (8)
MSI 45A	Lowermost Unit	hsg EMII	0.703267 (3)	0.512854 (2)	19.339 (1)	15.636 (1)	39.055 (2)	0.282910 (9)
NZS14	Lowermost Unit	hsg EMII	0.703325 (5)	0.512871 (3)	19.337 (1)	15.642 (1)	39.073 (2)	

Please cite this article as: Timm, C., et al., Temporal and geochemical evolution of the Cenozoic intraplate volcanism of Zealandia, Earth-Science Reviews (2009), doi:10.1016/j.earscirev.2009.10.002

Table 2 (*continued*)

Sample number	Location	Group	$^{87}Sr/^{86}Sr$	$^{143}Nd/^{144}Nd$	$^{206}Pb/^{204}Pb$	$^{207}Pb/^{204}Pb$	$^{208}Pb/^{204}Pb$	$^{176}Hf/^{177}Hf$
Canterbury: Timaru and Geraldine Basalt								
MSI 6A	Timaru basalt	hsg EMII	0.703744 (3)	0.512831 (3)	18.858 (2)	15.611 (1)	38.711 (4)	0.282895 (8)
MSI 8A	Geraldine basalt	hsg EMII	0.703575 (5)	0.512893 (2)	19.169 (1)	15.614 (1)	38.928 (2)	
Otago: Dunedin Volcano								
30-10-02-1	Aramoana	lsg	0.702858 (5)	0.512922 (3)	19.977 (1)	15.635 (1)	39.447 (2)	
12-11-02-3	Mt. Holmes Organ Pipes	lsg	0.702888 (4)	0.512919 (3)	19.849 (1)	15.640 (1)	39.389 (2)	0.282967 (6)
30-11-02-1	Pilot Point	lsg	0.702900 (4)	0.512915 (2)	20.231 (1)	15.656 (1)	39.697 (3)	
OU22636	Mt. Cargill	lsg	0.702949 (3)	0.512897 (2)	19.980 (1)	15.641 (1)	39.511 (1)	
OU22855[a]	St. Clair beach	lsg	0.702913 (5)	0.512913 (5)	20.074 (1)	15.658 (1)	39.598 (3)	0.282992 (7)
LSI22[a]	Allans beach	lsg	0.703032 (6)	0.512871 (8)	20.189 (3)	15.664 (2)	39.802 (5)	0.282967 (7)
MSI 87	Cape Saunders rd	lsg	0.703029 (5)	0.512905 (2)	19.925 (1)	15.649 (1)	39.416 (2)	
MSI 90A	Taiaroa Head	lsg	0.702855 (5)	0.512914 (3)	20.146 (1)	15.637 (1)	39.596 (1)	
MSI 95	Mt. Cargill rd	lsg	0.702986 (5)	0.512902 (4)	20.098 (1)	15.646 (1)	39.563 (1)	
Otago: Waipiata Volcanic Field								
OU54926[a]	Lookout Bluff	lsg	0.703261 (7)	0.512887 (7)	19.253 (2)	15.618 (2)	38.935 (3)	0.282965 (7)
LST1[a]	Conical Hill	lsg	0.702895 (8)	0.512858 (9)	20.349 (5)	15.644 (3)	40.101 (7)	0.282988 (7)
Otago: Waiareka–Deborah Formation								
LSI7[a]	Bridge Point	hsg EMII	0.703387 (4)	0.512838 (3)	18.999 (1)	15.628 (1)	38.735 (2)	0.282899 (7)
OU54929[a]	1 km SE of Maheno	hsg EMII	0.703210 (7)	0.512861 (6)	19.248 (2)	15.636 (1)	38.888 (4)	0.282905 (8)
Westland: Otitia Basalt								
MSI 63A	Otitia Basalt	lsg	0.704956 (2)	0.512825 (2)	19.730 (2)	15.625 (1)	39.739 (3)	0.282921 (7)
MSI 63E	Otitia Basalt	lsg	0.704627 (5)	0.512814 (3)	19.794 (2)	15.629 (1)	39.716 (4)	
Westland: Arnott Basalt								
MSI 65A	Along the coastline	lsg		0.512866 (2)	20.214 (3)	15.648 (2)	39.937 (5)	
MSI 66	Along the coastline	lsg	0.703335 (3)	0.512861 (2)	20.340 (3)	15.643 (3)	40.027 (6)	0.282960 (11)
Westland: Alpine Dike Swarm								
MSI 69B	Alpine Dike Swarm	lsg	0.703253 (3)	0.512846 (2)	20.616 (1)	15.657 (1)	40.337 (1)	
MSI 70B	Alpine Dike Swarm	lsg	0.703679 (2)	0.512851 (2)	20.170 (1)	15.649 (1)	39.929 (1)	
MSI 71A	Alpine Dike Swarm	lsg	0.703483 (5)	0.512854 (3)	20.443 (1)	15.651 (1)	40.163 (1)	
Lake Hawea 3	Alpine Dike Swarm	lsg	0.704050 (2)	0.512862 (2)	20.221 (1)	15.650 (1)	39.976 (2)	

Sr, Nd, Pb, Hf and O isotope data from Banks Peninsula are available in Timm et al. (2009).
All sample numbers and names of SO168 and SO169 samples are working names.
Abr.: lsg = low-silica group, hsg = high-silica group.
[a] Sr, Nd, Pb isotope data were taken from Hoernle et al. (2006).

4.2. Geochemistry of Cenozoic intraplate volcanic rocks from Zealandia

4.2.1. Major and trace elements

Major and trace element analyses are given in Supplementary File 1 and isotope data are given in Table 2.

Volcanic rocks from Zealandia range from nephelinite/basanite through phonolite, and alkali basalt through trachyte and peralkaline rhyolite, with minor occurrences of tholeiites and basaltic andesites (rock classification after Le Maitre, 2002; Fig. 5A). The studied mafic samples (MgO>5 wt.%) range from tholeiite–basaltic andesite to alkali basalt–mugearite to basanite–tephrite to nephelinite (Fig. 5B). On binary diagrams with SiO_2 (not shown), the samples show moderate to good positive correlations with Al_2O_3, Na_2O, K_2O and negative correlations with TiO_2, FeO^t, CaO, which can be explained by fractional crystallization of the common mineral phases olivine, orthopyroxene, clinopyroxene and plagioclase. Based on SiO_2 content versus alkalies, the most mafic volcanic rocks (nephelinites–basanites–alkali basalts–tholeiites) can be divided into a low-silica (SiO_2<46 wt.%) and a high-silica (SiO_2>46 wt.%) group, as defined by Hoernle et al. (2006) (Fig. 5B). More evolved samples within a group can be derived from more mafic rock compositions in the group through fractional crystallization. At a given MgO content, the low-silica group generally has higher TiO_2, FeO^t, CaO and Na_2O in contrast to the high-silica group, but there is almost complete overlap in Al_2O_3 of both groups. On the SiO_2 vs. FeO^t diagram, three samples with MgO>6 wt.% from Northland fall beneath the main array formed by the high-silica group rocks to lower FeO^t contents. Compared to the high-iron, high-silica samples, the low-iron, high-silica samples also generally extend to the lowest SiO_2, TiO_2 and K_2O but to the highest Al_2O_3 at a given MgO content (Fig. 6A–H).

Most mafic volcanic rocks from Zealandia (MgO>5 wt.%) show similar incompatible-element characteristics to ocean island basalts (OIB) on multi-element diagrams, with typical negative anomalies at Pb and K and positive anomalies at Nb and Ta (Fig. 7). The anomalies for Nb, Ta, Pb and K generally become more pronounced in rocks with lower silica contents (e.g. higher Nb/La, Nb/K, Ce/Pb and Nd/Pb). The low-silica rocks also have higher Zr/Hf and Nb/Ta. In the more silica-rich rocks, the OIB-type patterns are smoother approaching enriched (E) MORB-type signatures, except that the HREE elements form steep rather than flat patterns, as is characteristic of enriched E-MORB. In addition, the high-silica rocks have higher fluid-mobile to less fluid-mobile (e.g. U/La, Rb/Zr, Ba/Y, Sr/Nd, Pb/Nd) and lower more to less incompatible-element ratios (e.g. Zr/Hf, (Zr, Hf)/Nb, Zr/Y, (Nb, Ta)/Th, Nb/La, La/Sm, (Sm, Gd)/Yb). Compared to the high-iron, high-silica samples, the low-iron, high-silica samples have lower HREE and MREE, but higher HREE and Y abundances, reflected in, for example, lower Tb/Yb, Sm/Yb and La/Yb ratios.

4.2.2. Sr–Nd–Hf–Pb isotope data

The mafic Cenozoic volcanics have relatively low to moderate $^{87}Sr/^{86}Sr$ (0.7027–0.7050) and moderate to high $^{143}Nd/^{144}Nd$ (0.5128–0.5131) and $^{176}Hf/^{177}Hf$ (0.2829–0.2831). Lead isotope ratios reveal a broad range: $^{206}Pb/^{204}Pb$ = 18.62–20.67, $^{207}Pb/^{204}Pb$ = 15.54–15.72 and $^{208}Pb/^{204}Pb$ = 38.27–40.34. The range in isotopic composition of the Cenozoic

Please cite this article as: Timm, C., et al., Temporal and geochemical evolution of the Cenozoic intraplate volcanism of Zealandia, Earth-Science Reviews (2009), doi:10.1016/j.earscirev.2009.10.002

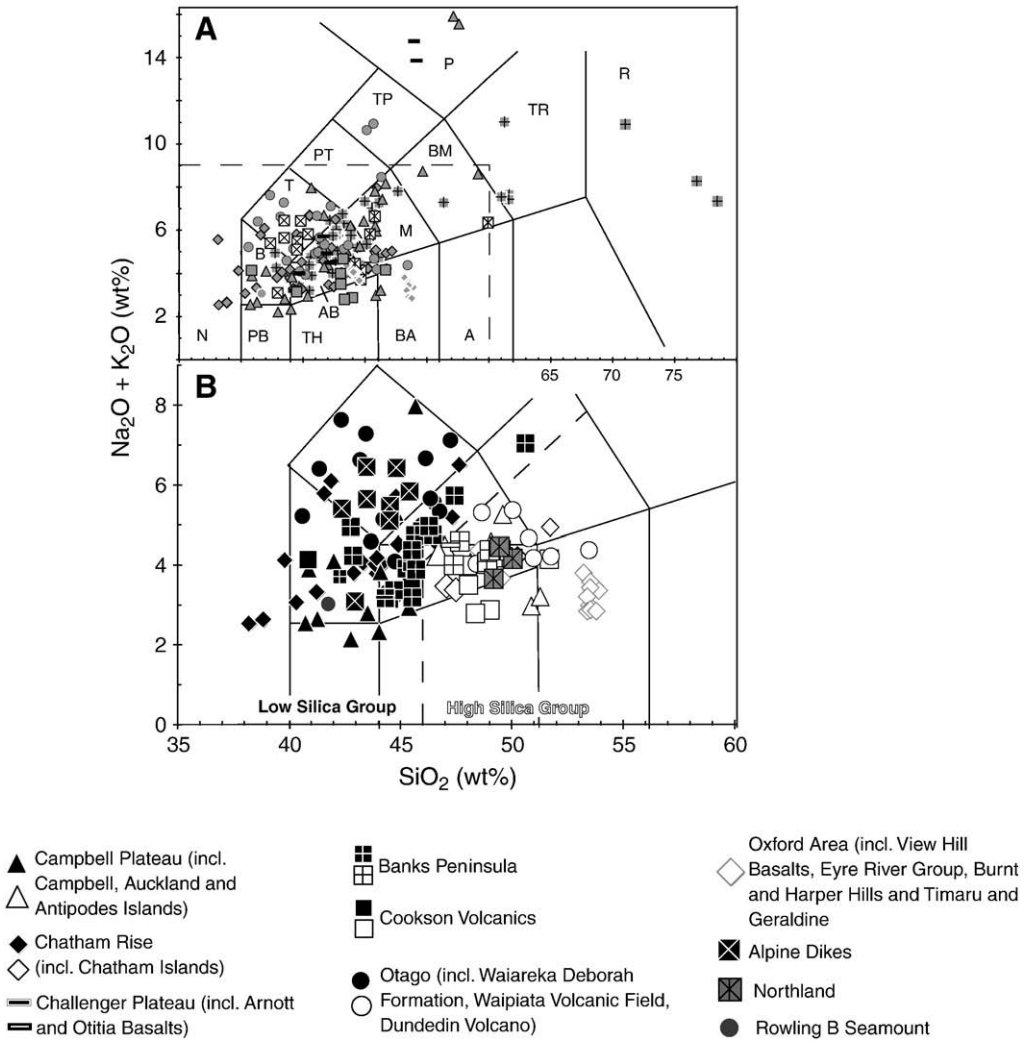

Fig. 5. SiO_2 vs total alkalies ($Na_2O + K_2O$) normalized to 100% on a volatile-free basis according to rock-type classification (Le Maitre, 2002). (A) Samples from Zealandia range from tholeiite through basaltic andesite to alkali basalt through trachyte and peralkaline rhyolite to basanite through phonolite to nephelinite (data from this study and the literature). (B) Mafic (MgO>5 wt.%) volcanic rocks from Zealandia from this study are divided into 1) high-silica, high-iron (white symbols; SiO_2>46 wt.%), 2) low-iron, high-silica (grey symbols) and 3) low-silica (black; SiO_2<46 wt.%) groups. Abbreviations: F = foidite, PB = picrobasalt, B = basanite, T = tephrite, PT = phono-tephrite, TP = tephri-phonolite, P = phonolite, TH = tholeiite, AB = alkali basalt, H = hawaiite, M = mugearite, BM = benmoreite, TR = trachyte, BA = basaltic andesite, A = andesite, D = dacite, R = rhyolite.

Zealandia intraplate volcanic rocks falls within the range of ocean island basalts. On isotope correlation diagrams, the data largely forms an array extending from MORB to HIMU, but a third enriched (EMII)-type component is also required (Figs. 8 and 9).

The low-silica Cenozoic intraplate volcanic rocks on Zealandia are characterized by HIMU-like compositions having radiogenic Pb isotope ratios (e.g. $^{206}Pb/^{204}Pb = 19.2–20.7$). Almost all low-silica samples have negative Δ7/4Pb, i.e. they plot beneath the Northern Hemisphere Reference Line (NHRL of Hart, 1984) and form a crude array between HIMU and MORB-type mantle components (Fig. 9A). The low-iron, high-silica basalts have E-MORB-like (e.g. Northland volcanic rocks) compositions and the high-iron, high-silica samples enriched (EMII-type) isotopic compositions on Sr–Nd–Hf–Pb correlation diagrams (Figs. 8A–B and 9A–C). The high-silica rocks trending towards an EMII-like component also show a systematic decrease of more- to less-incompatible and more- to less-fluid-mobile trace element ratios as silica content increases. All Cenozoic mafic volcanic rocks, however, generally have less radiogenic Pb and Sr and more radiogenic Nd and Hf, compared to the Cretaceous volcanic rocks (Tappenden, 2003; Hoernle et al., 2005), but more radiogenic Pb and Sr and less radiogenic Nd and Hf isotopic compositions than Pacific N-MORB.

5. Discussion

We begin by reviewing the Late Cretaceous volcanism on Zealandia and the adjacent Hikurangi Plateau and then discuss the Cenozoic volcanism.

5.1. Late Cretaceous magmatism on Zealandia

Late Cretaceous magmatism on Zealandia has been attributed primarily to the end of subduction (Waight et al., 1998a; Tappenden, 2003) and subsequent development of an extensional regime (Barley and Weaver, 1988; Weaver et al., 1994). For the period 110–95 Ma, a transition from igneous source I-type to alkaline A-type intrusive rocks, together with the emplacement of mafic dikes, is reflected in rocks of Zealandia and Marie Byrd Land, and has been interpreted to record the transition from subduction to an extensional tectonic regime (e.g. Waight et al., 1998a; Storey et al., 1999).

Igneous activity linked to continental rifting (i.e. after subduction but before seafloor spreading) lasted for ~20 million years with an apparent peak in activity between 100 and 90 Ma represented by intrusions of the Tapuaenuku and Mandamus Igneous Complexes (Baker et al., 1994; Tappenden, 2003), the Lookout and Gridiron

Please cite this article as: Timm, C., et al., Temporal and geochemical evolution of the Cenozoic intraplate volcanism of Zealandia, Earth-Science Reviews (2009), doi:10.1016/j.earscirev.2009.10.002

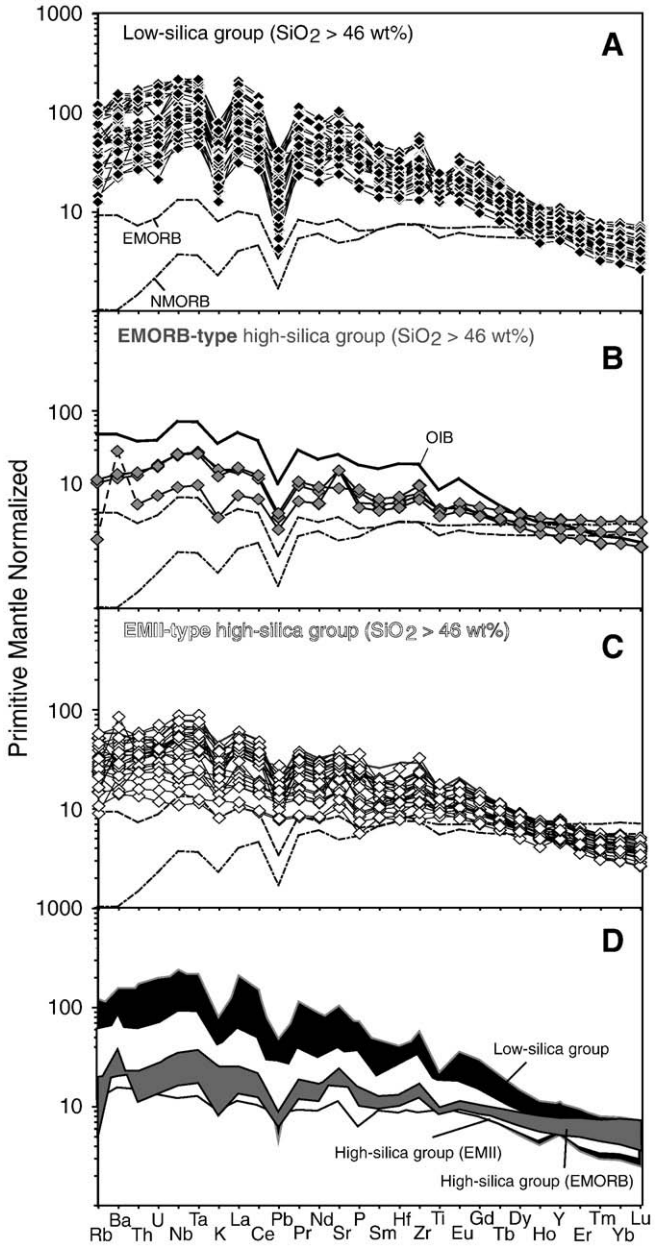

Fig. 6. Multi-element diagrams normalized to primitive mantle (Hofmann, 1988) of mafic (MgO>5 wt.%) Zealandia intraplate lavas: (A) patterns with the black diamonds belong to the low-silica group volcanic rocks (SiO_2<46 wt.%); (B) patterns with grey diamonds belong to the low-iron, high-silica group (SiO_2>46 wt.%), (C) patterns with white diamonds represent the high-iron, high-silica group volcanic rocks, and (D) the fields for the low-silica (black), low-iron, high-silica (grey) and high-iron, low-silica (white) volcanic rocks. For comparison, average ocean–island basalt (OIB), enriched mid-ocean-ridge basalt (E-MORB) and normal mid-ocean-ridge basalt (NMORB) patterns after Sun & McDonough (1989) are also shown.

Volcanics and large seamounts on the adjacent Hikurangi Plateau (Hoernle et al., 2003, 2005). These Late Cretaceous igneous rocks have HIMU-like trace element and isotopic compositions (Tappenden, 2003; Hoernle et al., 2005; Panter et al., 2006). Decompression melting of asthenospheric upwelling beneath the thinned lithosphere is a possible mechanism for generating volcanism beneath areas that underwent major continental extension during the Late Cretaceous. Seafloor spreading between Zealandia and eastern Australia and West Antarctica began at ~84 Ma, coinciding with the emplacement of the Hohonu Dike Swarm (Waight et al., 1998b). The HIMU-type geochemical characteristics of the entire age range of Late Cretaceous volcanism (c. 100–80 Ma) on the Hikurangi Plateau, South Island and Chatham Island could be related to a HIMU plume, proposed to have been located beneath Marie Byrd Land, that may have triggered the final phase of breakup of Gondwana at c. 107 Ma (Weaver et al., 1994; Hart et al., 1997; Storey et al., 1999; Panter et al., 2000, 2006).

5.2. Cenozoic volcanism

Cenozoic volcanism was widespread and essentially continuous across Zealandia and generally characterized by low volumes and predominantly alkaline composition. The frequency of larger volcanic centers (≥100 km^3) with primarily tholeiitic to alkali basaltic compositions, in many cases forming composite shield volcanoes, appears to have crudely increased throughout the Cenozoic: Arnott Basalt Event (c. 65–61 Ma), Cookson Volcanic Event (31–26 Ma), Auckland Islands Volcanoes (c. 17–15 Ma), Dunedin Volcano (c. 16–12 Ma), Lyttelton Volcano (c. 12–10 Ma), Akaroa Volcano (9–6 Ma), Campbell Volcano (c. 8–7 Ma), and Antipodes Volcano (<1 Ma) (Fig. 4). As is clear from a detailed study of the well-exposed Banks Peninsula Volcanoes (Lyttelton and Akaroa), volcanic activity formed the voluminous composite shield volcanoes generally over less than 2 million years, followed by prolonged small-volume, late-stage volcanism (Timm et al., 2009). Interestingly the composite shield volcanoes of Dunedin (~16–12 Ma) and Banks Peninsula (~12–6 Ma) were formed towards the end of diffuse volcanic activity that took place over a much larger area around the shield volcanoes: the Waipiata Volcanic Field (~25–11 Ma) and offshore volcanism in the vicinity of the Dunedin Volcano and widespread Miocene volcanism around Banks Peninsula (in the Oxford area and offshore of the Banks Peninsula on the Chatham Rise; ~26–12 Ma). Therefore it appears that melting and magma production increased significantly and became more focused at the end of longer-lived diffuse magmatic events, resulting in the formation of composite shield volcanoes (Hoernle et al., 2006; Timm et al., 2009).

We can now demonstrate that volcanism with intraplate geochemical compositions occurred over much, if not most, of the Cenozoic in several different locations on Zealandia (Fig. 2). We will first review the *onshore volcanic activity*. In Canterbury, volcanic activity at View Hill took place between ~53 and 48 Ma, the Cookson Volcanics were erupted between ~31 and 26 Ma, volcanism in the Oxford area ranges in age from ~25 Ma to ~12 Ma (this study and Sewell and Gibson, 1988), Banks Peninsula shield volcanoes were active between ~12.5 and 7 Ma (Timm et al., 2009 and references therein) and volcanism at Timaru and Geraldine occurred at ~2.5 Ma. In Otago, Paleocene volcanic activity has been recorded in the Endeavour-1 drillhole just offshore of Oamaru. On land, the oldest Waiareka–Deborah volcanism is Late Eocene (~40–34 Ma), followed by the Waipiata Volcanic Field volcanism, which was low-volume but almost continuous from ~25 to ~11 Ma with formation of the Dunedin shield volcano during its final stages (~16–12 Ma) (this study and Hoernle et al., 2006; Coombs et al., 2008). The Alpine dike swarm in Westland on the Pacific Plate (west of Otago) overlaps in age with the older part of the Waipiata volcanism and may be an extension of this volcanism. The part of Westland on the Australian Plate only forms a thin sliver of land between the Southern Alps mountain range and the coast but records at least two volcanic episodes, in addition to the Alpine dikes, which are difficult to age date due to their metamorphosed nature: 1) the early Paleozoic Arnott Basalts, which may have formed a shield volcano in particular if it is accepted that the submarine volcanism offshore of the Arnott Basalts were formed during the same event, and 2) the Late Oligocene Otitia basalts (28.6 ± 0.3 Ma). Due to the occurrence of these volcanic rocks on the Australian Plate, they are likely to have formed as much as 500 km to the south of the part of Westland on the Pacific Plate (e.g. Sutherland, 1995). On the North Island of New Zealand in the Northland and Auckland areas, volcanism with intraplate geochemical compositions was active from the mid Miocene to Recent (~10 Ma to

Please cite this article as: Timm, C., et al., Temporal and geochemical evolution of the Cenozoic intraplate volcanism of Zealandia, Earth-Science Reviews (2009), doi:10.1016/j.earscirev.2009.10.002

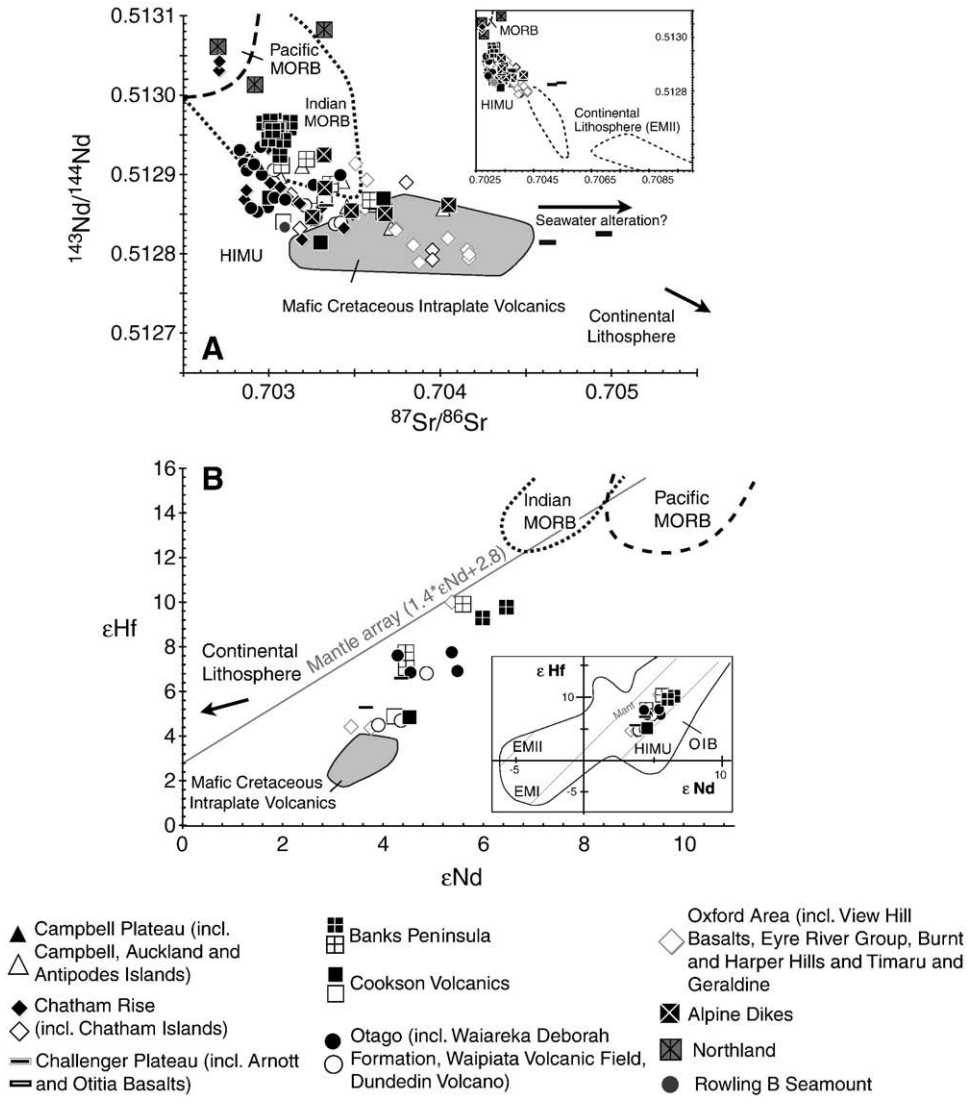

Fig. 7. On (A) $^{87}Sr/^{86}Sr$ versus $^{143}Nd/^{144}Nd$ and (B) εNd versus εHf diagrams, the mafic (MgO > 5 wt.%) Cenozoic volcanic rocks define an array between HIMU and Pacific MORB. The higher $^{87}Sr/^{86}Sr$ isotope ratios, compared to Nd isotope ratios, of several samples from the Challenger Plateau and one sample from Northland may reflect sea/groundwater contamination. References fields and lines are from Tappenden (2003), Hoernle et al. (2005), Storey et al. (1999), Zindler and Hart (1986) and Blichert-Toft and Albarede (1997). White fields in the inset represents composition expected of the Zealandia lithosphere (similar in composition to Cretaceous subduction-related rocks from Mt. Somers, Takahe (granite) and Stuttgart (schist) seamounts, and mafic dikes from Marie Byrd Land, Antarctica; Tappenden, 2003; Storey et al., 1999; Mortimer et al., 2006).

~500 years ago; this study and see summary in Cook et al., 2004). The earliest Cenozoic volcanic activity on the Subantarctic islands occurred on the Chatham Islands during the Eocene (Northern Volcanics; 41–35 Ma; Panter et al., 2006). In the Miocene volcanism was active on the Auckland (16.7 ± 1.2 to 15.2 ± 0.3 Ma; Hoernle et al., 2006), on the Campbell Islands (7.5 ± 0.3 to 6.6 ± 0.6 Ma; Hoernle et al., 2006) and on the Chatham Islands (Rangitihi volcanic group; c. 5 Ma; Panter et al., 2006). Pleistocene volcanic activity occurred on the Antipodes Islands (0.30 ± 0.11 to 0.17 ± 0.18 Ma), forming the youngest volcanic rocks on the Subantarctic islands.

Now we review the *offshore volcanic activity*. On the western and central Chatham Rise, volcanism has been recorded over most of the Cenozoic. The oldest volcanism on the central Chatham Rise, northwest and south of the Chatham Islands, was dated at 63.0 ± 0.6 and 56.5 ± 0.5 Ma, respectively. Our age of 32.8 ± 0.7 Ma from submarine volcanism just south of the Chatham Islands is within error of the age of 36.0 ± 4.2 Ma obtained for the intermediate episode of volcanism on the Chatham Islands (Panter et al., 2006). Two other volcanic centers south of the Chatham Islands yielded ages of 22 and 5.2 Ma, with the latter two ages falling within the range of the youngest episode of volcanism on the Chatham Islands (4.3–7.3 Ma) (Panter et al., 2006, and this study). Volcanism on the western Chatham Rise ranges from Early Miocene through Pliocene with different volcanic fields yielding ages of c. 22, 20, 14, 13, 9 and 3 Ma. Combined age data from the central and western Chatham Rise shows that volcanism took place in the Paleocene, Late Eocene/Early Oligocene and then was nearly continuous over the last 22 Ma with the largest gap in age dates during this time interval being ~6 Ma. The sparser record of sampled Paleocene through Oligocene volcanism could well represent the increased difficulty in obtaining samples from these older units due to possibly more extensive sedimentation covering the older volcanic rocks, as for example shown by seismic data of Uenzelmann-Neben et al. (2009).

The Campbell and Challenger Plateaus have not been sampled in as great a detail as the Chatham Rise. Nevertheless, volcanism on the Campbell Plateau has been dated at c. 39, 17–15, 8–7, 4–3, 0.8–0.2 Ma, overlapping largely with Late Eocene to Quaternary volcanism on the Chatham Rise. The only dated volcanism from the Challenger Plateau is from Mt. Spong, giving an age range of 38–36 Ma, overlapping within errors with volcanism in Otago (Waireka–Deborah volcanism,

Please cite this article as: Timm, C., et al., Temporal and geochemical evolution of the Cenozoic intraplate volcanism of Zealandia, Earth-Science Reviews (2009), doi:10.1016/j.earscirev.2009.10.002

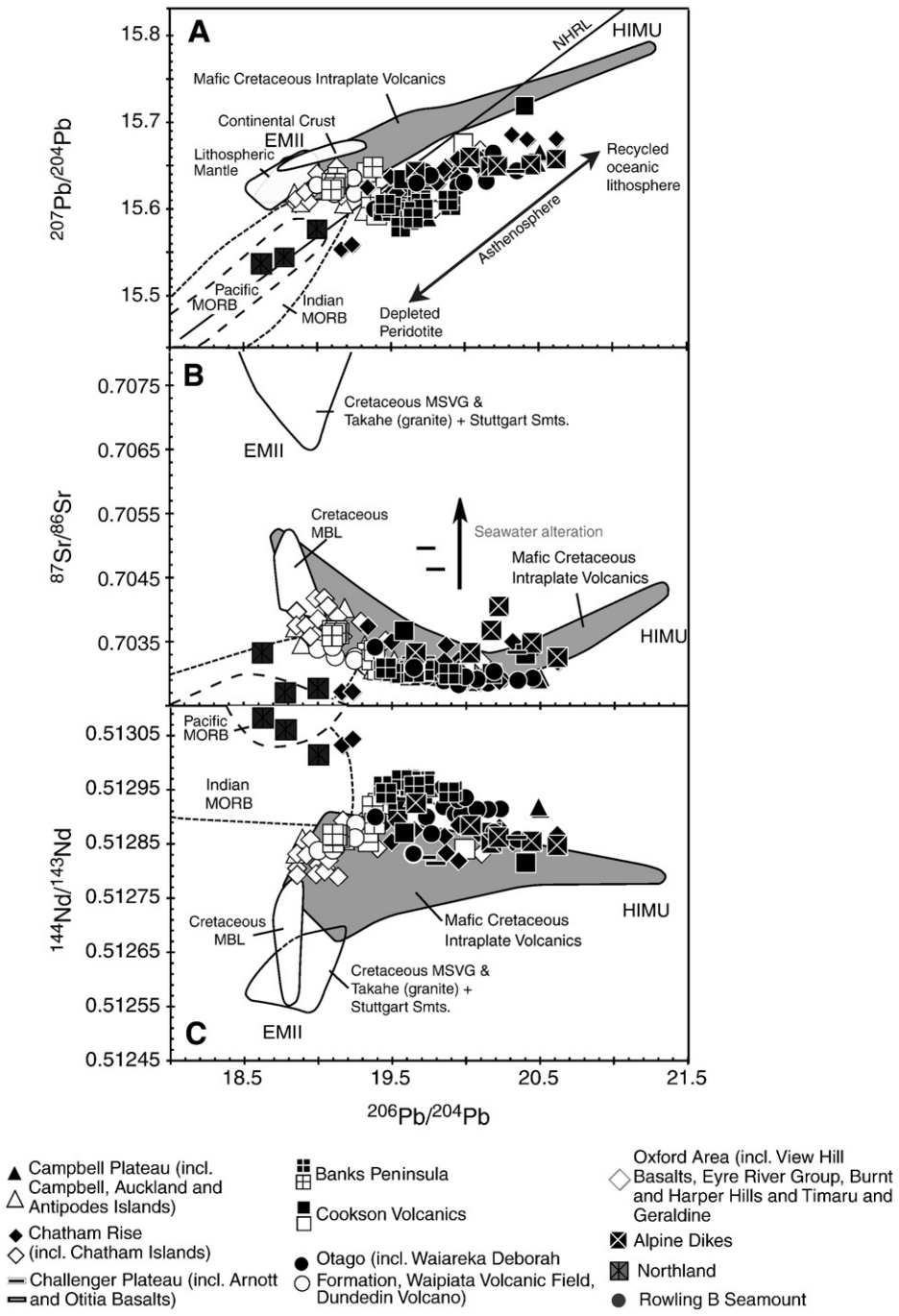

Fig. 8. $^{206}Pb/^{204}Pb$ versus $^{207}Pb/^{204}Pb$, $^{87}Sr/^{86}Sr$ and $^{143}Nd/^{144}Nd$ isotope correlation diagrams for mafic (MgO > 5 wt.%) Zealandia volcanic samples (including data from Hoernle et al., 2006 and Timm et al., 2009). The low-silica group samples have the most radiogenic Pb but intermediate Sr and Nd isotopic compositions, whereas the high-silica group extends from the low-silica volcanic rocks to relatively unradiogenic Pb isotopic ratios. The high-silica samples form two groups: 1) low-iron depleted group with unradiogenic Sr but radiogenic Nd isotope ratios with compositions similar to E-MORB, and 2) a high-iron enriched (EM II-type) group with relatively radiogenic Sr but unradiogenic Nd, which trends towards the composition expected of the Zealandia lithosphere (similar in composition to Cretaceous subduction-related rocks from Mt. Somers, Takahe (granite) and Stuttgart (schist) seamounts, and mafic dikes from Marie Byrd Land, Antarctica; Tappenden, 2003; Storey et al., 1999; Mortimer et al., 2006). The field for mafic Cretaceous Zealandia intraplate volcanic rocks is from Tappenden (2003) and Hoernle et al. (2005).

c. 40–34 Ma), on and south of the Chatham Islands (c. 36–33 Ma) and on the Campbell Plateau west of the Antipodes Islands (39 Ma). Finally, it is important to note that Cenozoic intraplate volcanism also took place on the Hikurangi Plateau (at Rowling Seamount), a fragment of a Cretaceous large igneous province.

In conclusion, volcanism within a given region on Zealandia not only took place during much of the Cenozoic, but also, at a given age, volcanism occurred over much of the micro-continent simultaneously. These observations are clearly not consistent with a plume hypothesis or with large-scale continental extension being the cause of the Cenozoic intraplate volcanism. As an alternative to these models, melting of volatile-rich lower lithosphere due to heat conduction from a hotter than normal asthenosphere has also been proposed to explain the intraplate volcanism on Zealandia and surrounding areas (Finn et al., 2005; Panter et al., 2006; Sprung et al., 2007). Although diffuse, low-volume volcanic activity forming monogenetic volcanic centers and fields and restricted dike and intrusive events could possibly be explained by lithospheric melting, such a model is not consistent with

Please cite this article as: Timm, C., et al., Temporal and geochemical evolution of the Cenozoic intraplate volcanism of Zealandia, Earth-Science Reviews (2009), doi:10.1016/j.earscirev.2009.10.002

the generation of large volumes of melts in relatively short time periods (several million years) as required to explain the larger magmatic events and composite shield volcanoes, such as the Arnott Basalts, Cookson Volcanics and the Dunedin, Lyttelton, Akaroa, Antipodes and possibly the Ross, Carnley and Campbell composite shield volcanoes. Finally, the geochemical similarity in major elements, trace elements and isotopes between the basalts of the composite shield volcanoes and those from monogenetic centers indicates that these two endmember types of Cenozoic volcanism (e.g. Hoernle et al., 2006) must be derived from similar sources and therefore places into question an exclusively lithospheric origin for the Cenozoic intraplate volcanism.

The cause of the Cenozoic intraplate volcanism on Zealandia remains controversial, and will therefore be evaluated in more detail in the following section.

5.3. Source characteristics of Cenozoic intraplate volcanic rocks from Zealandia

Although major and trace element and $^{206}Pb/^{204}Pb$ isotopic compositions of the mafic Cretaceous and Cenozoic intraplate volcanic rocks (MgO>5 wt.%) largely overlap, the Cenozoic lavas generally have less radiogenic $^{87}Sr/^{86}Sr$, $^{207}Pb/^{204}Pb$ and $^{208}Pb/^{204}Pb$ but more radiogenic Nd and Hf isotopic compositions, plotting between the field for the Cretaceous volcanic rocks and Pacific N-MORB. Therefore the composition of the Cenozoic volcanic rocks could be, at least in part, explained by mixing of Cretaceous-type melts with a MORB source.

As noted above, the mafic volcanic rocks from Zealandia can be divided into high (SiO_2>46 wt.%)- and low (SiO_2<46 wt.%)-silica groups. Compared to the high-silica group, the low-silica volcanic rocks generally have higher TiO_2, FeO^t, CaO, higher abundances of incompatible elements (e.g., Nb, Ta, Zr, Hf, Rb, Sr, U), higher more- to less-incompatible-element ratios (La/Sm, (Sm, Gd)/Yb, (Nb, Zr)/Y, Th/(Nb, Ta), Nb/(Zr, Hf), Nb/La), higher Zr/Hf and Nb/Ta and lower fluid-mobile to fluid-immobile element ratios (U/La, Ba/Zr, Rb/Nd, (K, Pb, Sr)/Nb). On isotope correlation diagrams, the low-silica group rocks form an array between MORB and the HIMU mantle endmember and have the most HIMU-like compositions of the Cenozoic volcanic rocks.

The high-silica lavas can be subdivided based on FeO^t content. The low-iron, high-silica rocks have the most depleted incompatible-element compositions. The high-iron, high-silica samples, on the other hand, have the highest fluid-mobile to fluid-immobile element abundances (e.g. U/La, Ba/Zr, Rb/Nd, (K, Pb, Sr)/Nb) and higher Hf/Nb, Zr/Nb and Th/Ta but lower Sm/Yb. Both low- and high-iron groups generally have less radiogenic Pb isotope ratios. The low-iron group samples trend towards a MORB (DMM)-like component with highest Nd and Hf isotope ratios, whereas the high-iron group trend towards an enriched (EMII)-type component with the least radiogenic Nd and Hf and more radiogenic Sr isotope ratios (Figs. 8 and 9). In summary, the geochemistry of Cenozoic volcanic rocks throughout Zealandia requires the presence of at least three components (see Figs. 8 and 9): 1) low-silica, HIMU-type component, 2) low-iron, high-silica, MORB (or DMM)-like component and 3) high-iron, high-silica, EMII-type component (data from this study and Barreiro and Cooper, 1987; Price et al., 2003; Cook et al., 2004; Hoernle et al., 2006; Panter et al., 2006; Sprung et al., 2007; Timm et al., 2009). These systematic differences in geochemical composition suggest fundamental differences in the formation of the groups, which will be evaluated below.

5.4. Low-silica mafic volcanic rocks — partial melting of upwelling heterogeneous asthenosphere

The distinct isotopic compositions of the low-silica Cenozoic intraplate volcanic rocks from Zealandia clearly indicate that they are largely derived from different sources than the high-silica volcanic rocks (Hoernle et al., 2006; Timm et al., 2009). The low-silica volcanic rocks are characterized by HIMU-like compositions having radiogenic Pb isotope ratios (e.g. $^{206}Pb/^{204}Pb = 19.2–20.7$) and form a crude array between HIMU (or Cretaceous intraplate volcanic rocks on Zealandia) and MORB-type mantle components. Below we discuss what the major and trace element and isotopic compositions of these rocks can tell us about their origins.

Compared to experimentally-generated melts of peridotite (Hirose and Kushiro, 1993; Dasgupta et al., 2007), garnet pyroxenite (Hirschmann et al., 2003), eclogite (Kogiso and Hirschmann, 2006; Dasgupta et al., 2006) and hornblendite (Pilet et al., 2008) (see Fig. 6), the low-silica group compositions lie between the fields for high-pressure experimental melts of eclogite (at 30–50 kb and 1470–1600 °C) and eclogite + CO_2 (at 30 kb and 1315–1400 °C) and peridotite ± CO_2 (at 30 kb and 1300–1600 °C), consistent with derivation from a lithologically-mixed source (e.g. eclogite within a peridotitic matrix) at pressures ≥ 30 kb (≥ 100 km depth). Since the Zealandia lithosphere, except beneath the Southern Alps, is generally c.100 km (e.g. Molnar et al., 1999), the low-silica source appears to lie within the asthenosphere. High ratios of lighter to heavier heavy REE (e.g. Sm/Yb, Tb/Yb) and steep HREE patterns with negative slopes on multi-element diagrams in the low-silica group volcanic rocks are indicative of residual garnet, consistent with an eclogitic or garnet peridotitic source. High Zr/Hf (Fig. 11) of the low-silica melts provide additional support for eclogite in the source (Pertermann et al., 2004; Pfänder et al., 2007). The high Nb/Ta (16–26) and low Zr/Sm (20–36) are also consistent with partial melting of rutile-bearing eclogite (Foley et al., 2002).

Panter et al. (2006) has proposed that the source of some Cenozoic alkaline volcanic rocks may contain amphibole, which would imply a lithospheric source for at least some of the low-silica volcanic rocks (e.g. Class and Goldstein, 1997). Pilet et al. (2008) have pointed out that the high K_2O content of alkaline volcanic rocks is a general problem, which led them to propose melting of hornblendite to derive alkaline melts. It should be noted that only the experiments with hornblendite in the starting material generated melts with high K_2O. The MgO, FeO^t and Na_2O of these high-K_2O melts, however, are too low to explain the compositions of the low-silica group by melting of hornblendite (±clinopyroxene ± peridotite; Pilet et al., 2008) (Fig. 6). In addition, ratios of $(Zr/(Sm, Eu))_n$ (=normalized to primitive mantle ratios) and $((Th, U)/Ba)_n$ of >1 are also not consistent with an amphibole-bearing source based on the trace element data in Pilet et al. (2008). Therefore the high K_2O contents in the most mafic melts require a higher K_2O content in one of the starting (source) materials than used in the experiments. An alternative to amphibole in the source of these rocks is that low-silica melts are derived from recycled K (incompatible-element) enriched rocks, such as alkali basalts found on oceanic islands and seamounts, that are generally enriched in most incompatible elements compared to normal MORB tholeiites (Hémond et al., 2006), but that form silica-poor eclogite upon subduction. Of course, many other mantle enrichment scenarios can be envisaged to enrich the sources of intraplate volcanism in K and other incompatible elements.

Fig. 9. Diagrams showing (A–G) MgO vs. selected major elements and (H) SiO_2 vs. FeO^t for mafic samples (MgO>6 wt.%) of the Cenozoic Zealandia volcanic rocks. The following filters were applied to reject strongly altered rocks: H_2O>3 wt.%, CO_2>0.8 wt.% and MnO>0.25. All data are normalized to a 100% on a volatile-free basis. The high-silica group rocks have higher SiO_2 (as per definition) but also generally lower TiO_2, FeO^t, CaO and Na_2O relative to MgO. There is almost complete overlap in Al_2O_3 for both groups. The different fields show the compositional range of experimental melts: 1) the two dark grey fields include melts derived from dry (Kogiso and Hirschmann, 2006) and carbonated eclogite, respectively (Dasgupta et al., 2006), 2) the grey field includes melts of garnet pyroxenite (Hirschmann et al., 2003), 3) the light grey field includes melts of hornblendite (Pilet et al., 2008) and 4) the white fields include melts of peridotite with and without CO_2 (Hirose and Kushiro, 1993, Walter, 1998 and Dasgupta et al., 2007).

Please cite this article as: Timm, C., et al., Temporal and geochemical evolution of the Cenozoic intraplate volcanism of Zealandia, Earth-Science Reviews (2009), doi:10.1016/j.earscirev.2009.10.002

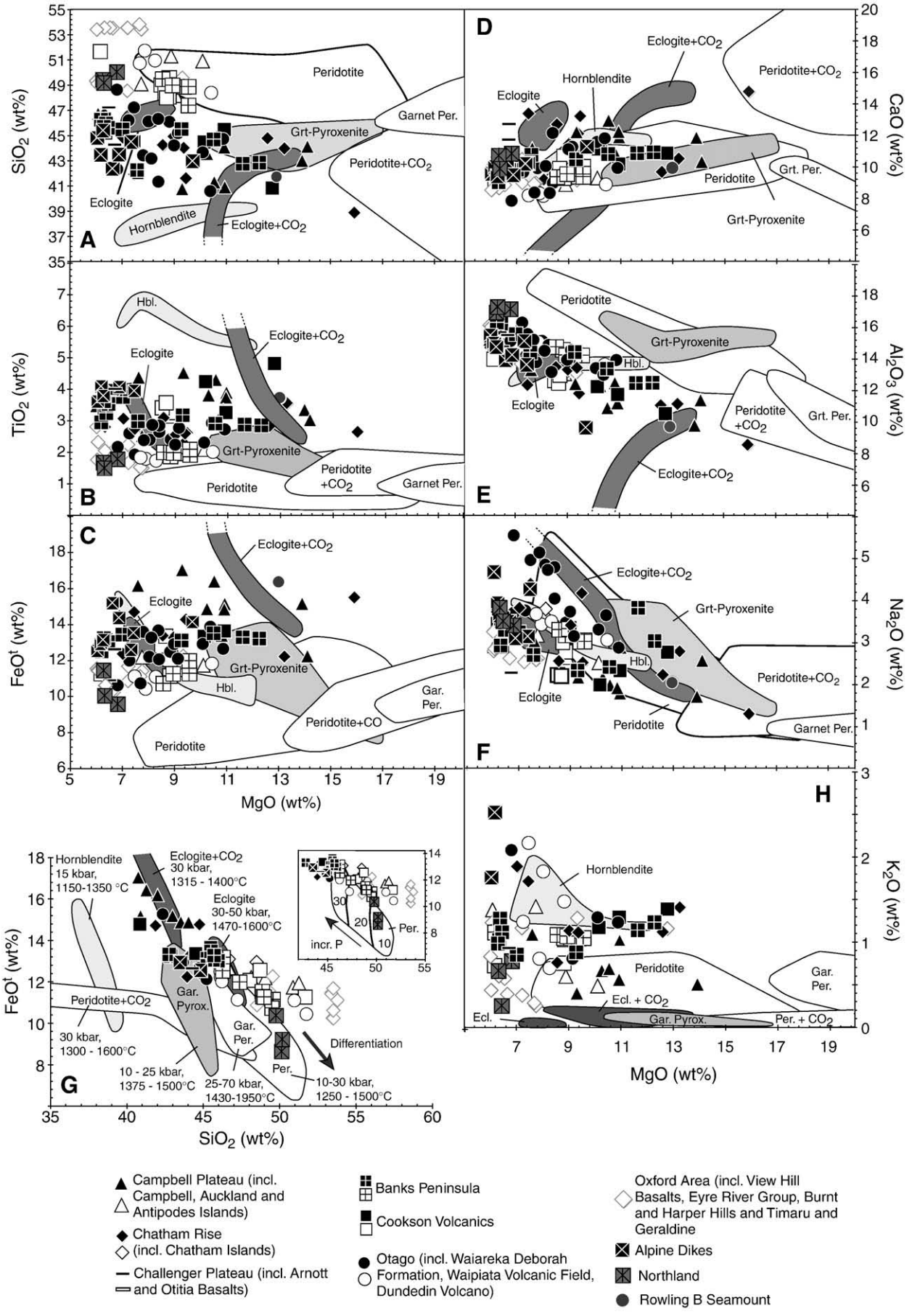

Please cite this article as: Timm, C., et al., Temporal and geochemical evolution of the Cenozoic intraplate volcanism of Zealandia, Earth-Science Reviews (2009), doi:10.1016/j.earscirev.2009.10.002

The most HIMU-type volcanic rocks were sampled at the Waipiata Volcanic Field, the Dunedin Volcano, the Cookson Volcanics, the Alpine dike swarm and the Chatham and Antipodes Islands (Barreiro and Cooper, 1987; Panter et al., 2006; Hoernle et al., 2006; this study). Some samples of the Alpine Dike Swarm trend towards the enriched (EMII-type) endmember (more radiogenic Sr and Nd isotopes, although less pronounced than in the high-silica group rocks), which suggests that interaction with the continental lithosphere (mantle and crust) may also play a role in some lavas of the low-silica group. Tappenden (2003), for example, showed that some of the Cretaceous Mandamus alkaline rocks with HIMU-like compositions on the South Island interpreted to be derived from asthenospheric depths, have been contaminated with Pahau (Torlesse Terrane) sediments. Lithospheric contamination, however, is not as obvious in the low-silica rocks, due in part to the higher concentrations of incompatible elements in these rocks.

In order to reconcile the major element with the trace element and isotope data for the low-silica rocks, Timm et al. (2009) concluded that the source of the low-silica rocks on Banks Peninsula was peridotite containing carbonated eclogite and was located in the asthenosphere, which agrees well with the results of the high-pressure melting experiments. Based on the chemistry of olivine phenocrysts in mafic volcanic rocks from the Canary Islands, Gurenko et al. (2009) showed that the HIMU-type component is derived from a peridotitic not eclogitic/pyroxenitic source, as is commonly inferred based on trace element and isotopic compositions. They proposed that older (>1 Ga) recycled oceanic crust is stirred into the largely peridotitic mantle. Timm et al. (2009) also proposed the derivation of mafic low-silica HIMU-type lavas from Banks Peninsula from predominately peridotite. In accordance with Dasgupta et al. (2006), who pointed out that different mantle components (e.g. peridotite, eclogite, pyroxenite) will melt at different temperatures and depths, they proposed that carbonated eclogite in the upwelling peridotitic asthenosphere will cross its solidus and melt first, metasomatizing the surrounding peridotite. The upwelling metasomatized peridotite melts at shallower depths, when the carbonated peridotite solidus is crossed, producing low-silica lavas with HIMU-type trace element and isotopic signatures. Such a model can also explain the geochemistry of the low-silica volcanic rocks from throughout Zealandia (Fig. 10).

In conclusion, since the mafic low-silica Cenozoic volcanic rocks plot between the fields for Pacific MORB and for Cretaceous volcanism on Zealandia and the Hikurangi Plateau, mixing of the Cretaceous lavas' mantle source with Pacific MORB-like upper mantle could explain the Sr–Nd–Hf and Pb isotope data ± some lithospheric contamination. We believe that the low $d^{18}O$ in olivine (<5.0) and major and trace element compositions of the low-silica volcanic rocks point to recycled crustal material in the source of these volcanic rocks, but cannot rule out that the low $d^{18}O$ results from interaction with hydrothermally-altered material in the volcanic edifice with similar radiogenic isotopic compositions.

5.5. High-silica mafic volcanic rocks — contribution of the lithosphere (mantle and crust)

Compared to the low-silica volcanic rocks, the mafic (MgO>5 wt.%), high-silica (SiO_2>46 wt.%) volcanic rocks (some alkali basalts, tholeiites and basaltic andesites) generally have lower FeO^t, TiO_2, CaO, incompatible-element concentrations and more- to less-incompatible-element ratios, e.g. Nb/(Zr, Hf), Sm/Yb, and higher fluid-mobile to fluid-immobile element ratios, e.g. U/La and U/Nb (Figs. 11 and 12). The high-silica rocks can be subdivided into high- and low-iron groups with the high-iron group having EMII-type isotopic compositions and the low-iron group having E-MORB-type compositions. At a given MgO content, the low-iron group also generally extends to the lowest SiO_2, TiO_2 and K_2O. They also have low concentrations of highly to intermediately incompatible

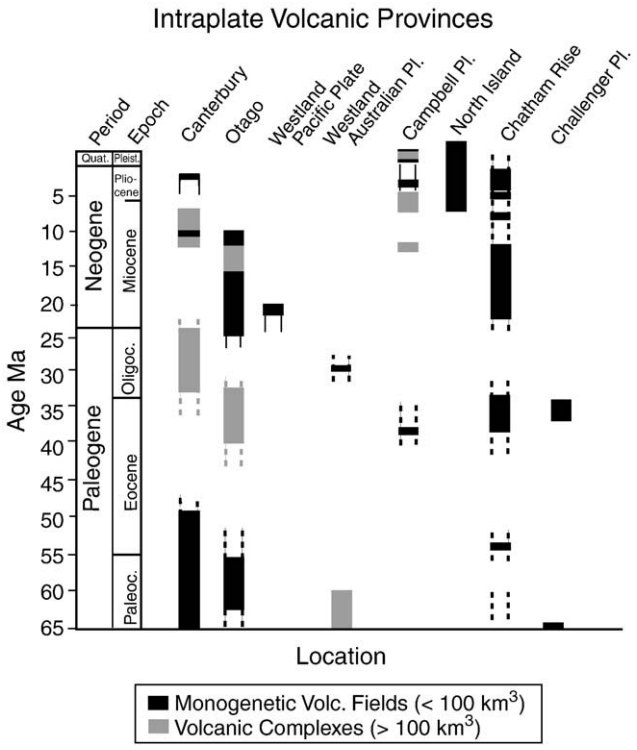

Fig. 10. Age distribution of the intraplate volcanic centers, based $^{40}Ar/^{39}Ar$ age data from Panter et al. (2006), Hoernle et al. (2006), Timm et al. (2009) and this study and <10 Ma K/Ar data from compilation in Cook et al. (2004). The closed areas represent the dated $^{40}Ar/^{39}Ar$ age range; dashed lines connect volcanism with gaps of ≤5 Ma and indicate an extended age range determined by the K/Ar, Rb/Sr and U/Pb methods (see text for details).

elements, but high HREE and Y abundances, reflected in, for example, lower Tb/Yb, Sm/Yb and La/Yb ratios.

In contrast to the low-silica rocks, the major element composition of the high-silica rocks overlap with or lie on an extension of the field for melts derived from melting of peridotite at high pressure (Hirose and Kushiro, 1993), suggesting that the high-silica melts could be differentiated from peridotitic melts (see Fig. 6). Based on the high-pressure experimental melting of dry peridotite (Hirose and Kushiro, 1993), the low FeO^t and SiO_2 of the low-iron subgroup overlaps the field for dry, peridotite-derived melts formed at pressures of ~10–15 kb and temperatures of 1250–1400 °C, whereas the high-iron subgroup overlaps the field for peridotite partial melts formed at ~20–30 kb at temperatures of 1350–1500 °C (Fig. 6G). The trend in the high-iron, high-iron group towards increasing SiO_2 and decreasing FeO^t reflects fractionation of olivine and Fe–Ti oxides. The generally higher contents of TiO_2, K_2O and highly- to intermediately incompatible elements of the high-iron subgroup suggests derivation from a more enriched source and/or lower degrees of partial melting. In summary, the high-iron, high-silica group of lavas appears to have generally formed at greater depths (~65–100 km) through lower degrees of melting than the low-iron group, which appears to have formed at shallower depths (~35–50 km) by generally greater degrees of melting. The pressures and temperatures of formation estimated for the low-iron group are similar to those for MORB.

Previously it has been proposed that high-silica rocks from Otago, Banks Peninsula and some of the Subantarctic islands were likely to have originally been derived from a sublithospheric source with depleted (similar to E-MORB) compositions that were subsequently contaminated in the crust and/or lithospheric mantle, geochemically enriched during subduction when Zealandia was part of the Gondwana margin in the Mesozoic (Hoernle et al., 2006; Timm et al., 2009). Original derivation from a depleted (E-MORB-type)

Please cite this article as: Timm, C., et al., Temporal and geochemical evolution of the Cenozoic intraplate volcanism of Zealandia, Earth-Science Reviews (2009), doi:10.1016/j.earscirev.2009.10.002

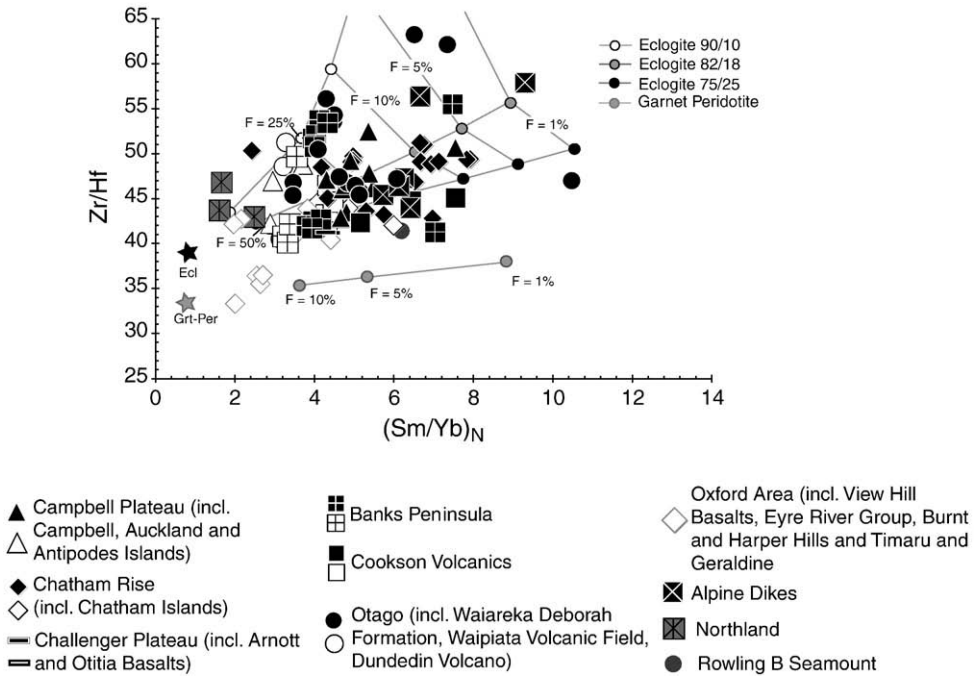

Fig. 11. $(Sm/Yb)_N$ versus Zr/Hf of mafic (MgO>6 wt.%) Cenozoic volcanic rocks. The grey dots indicate the composition of smaller degree partial melts of garnet peridotite. The parental garnet peridotite composition is denoted by the light grey star. The curves connected by the smaller black, grey and white dots represent increasing degrees of partial melting of eclogite with different clinopyroxene (first number) and garnet (number after the slash) mineral modes (in wt.%), as indicated in the legend. The parental eclogite composition is denoted by the black star. The grey lines indicate the fraction (F) of melt produced. Increasing $(Sm/Yb)_N$ ratios reflect increasing garnet signature, whereas increasing Zr/Hf indicates an increasing contribution of pyroxenite and/or eclogite to the partial melt. Modeling parameters are taken from Pertermann et al. (2004), except for slightly higher Zr (75 ppm) for the eclogite and slightly lower Zr (8 ppm) for the garnet peridotite composition. After our model, high degrees of partial melts (up to 50%) of eclogite are required to explain the Zr/Hf and $(Sm/Yb)_N$ ratios of mafic and silica-deficient lavas from Zealandia.

sublithospheric source, however, was not actually observed but only inferred from the incompatible element and isotope systematics. Of the high-iron, high-silica (EMII-like) subgroup, the Timaru basaltic andesites have the lowest incompatible-element abundances (similar to E-MORBs). These basaltic andesites with MgO = 7 wt.% do not have primitive compositions and have clearly undergone some differentiation. Since both crystal fractionation and lithospheric contamination (mantle and crust) would have increased the abundances of the incompatible elements, the incompatible-element abundances in the parental melts must have been even lower, leading to the interpretation that the parental melts were derived through high degrees of melting of a relatively depleted peridotitic source (Hoernle et al., 2006). In addition, it was shown that lithospheric interaction could explain the enriched isotopic compositions of high-silica melts from Timaru and the Waiareka–Deborah formation, if the asthenospheric melts had E-MORB-like isotopic compositions. Although E-MORB-type isotopic compositions were not actually observed in any of the previously studied rocks, the data from the Northland volcanic rocks confirm the presence of depleted high-silica rocks with E-MORB-type isotopic compositions. The geochemical compositions of the Northland volcanic rocks strengthen the model that the enriched high-silica volcanic rocks were formed through high degrees of melting of depleted peridotite and then contaminated in the lithosphere.

The lavas from the Timaru area, View Hill, Waiareka–Deborah Formation and Lyttelton Volcano show the greatest influence of an enriched (EMII-type) subduction-related lithospheric component. The presence of crustal xenoliths in lavas from these areas (e.g. Coombs et al., 1986; Duggan and Reay, 1986; Timm et al., 2009) suggests that crustal interaction has occurred even in the high-silica rocks with the lowest incompatible-element concentrations. Sewell and Gibson (1988) pointed out that the entire Canterbury volcanics (incl. View Hill and Oxford volcanics and Timaru basalt) show a crustal imprint. On the other hand, the presence of hydrous minerals, such as kaersutite and phlogopite in mantle xenoliths of the Waiareka–Deborah Formation (Reay and Sipiera, 1987), suggest source metasomatism and thus the ascending lavas are also likely to have experienced interaction with such a metasomatized lithospheric mantle.

Combined O–Sr–Nd–Hf–Pb isotope data for the tholeiitic rocks from Lyttelton Volcano on Banks Peninsula were explained by interaction of asthenospheric melts with the lithosphere (mantle and crust), especially of the oldest lavas (Timm et al., 2009). The enriched signature in the lavas of Banks Peninsula, however, cannot simply be created by assimilating continental crust, but also requires significant interaction with the lithospheric mantle, containing subduction-related pyroxenitic components (Timm et al., 2009). In conclusion, since the lithospheric mantle will no doubt have enriched domains with similar compositions to Cretaceous and older subduction-zone lavas that passed through the lithosphere on their way to the surface, it is extremely difficult, if not impossible, to distinguish between lithospheric mantle and crustal contamination. Even combined studies of O and radiogenic isotopes such as Sr–Nd–Pb–Hf cannot always unambiguously distinguish between contamination in these two parts of the lithosphere, since eclogitic components in the asthenosphere (derived from recycled hydrothermally-altered oceanic crust) that contribute to the formation of the parental magmas can have variable and lower $\delta^{18}O$ than the ambient peridotitic MORB-source mantle (e.g. Turner et al., 2007). In addition, substantial crustal contamination is required of mantle magmas with low $\delta^{18}O$ to generate $\delta^{18}O$ above typical upper mantle values (Timm et al., 2009). Finally, assimilation of hydrothermally-altered crust can also lower $d^{18}O$, making the interpretation of O isotope data partially difficult, as noted above.

In order to test further if the enriched (EMII-type) signatures of most high-silica rocks could reflect lithospheric interaction, we use the composition of the Late Cretaceous (c. 90–98 Ma) Mt. Somers Volcanic Group (data from Tappenden, 2003; Mortimer et al., 2006) as a potential endmember for the composition of the lithosphere,

Please cite this article as: Timm, C., et al., Temporal and geochemical evolution of the Cenozoic intraplate volcanism of Zealandia, Earth-Science Reviews (2009), doi:10.1016/j.earscirev.2009.10.002

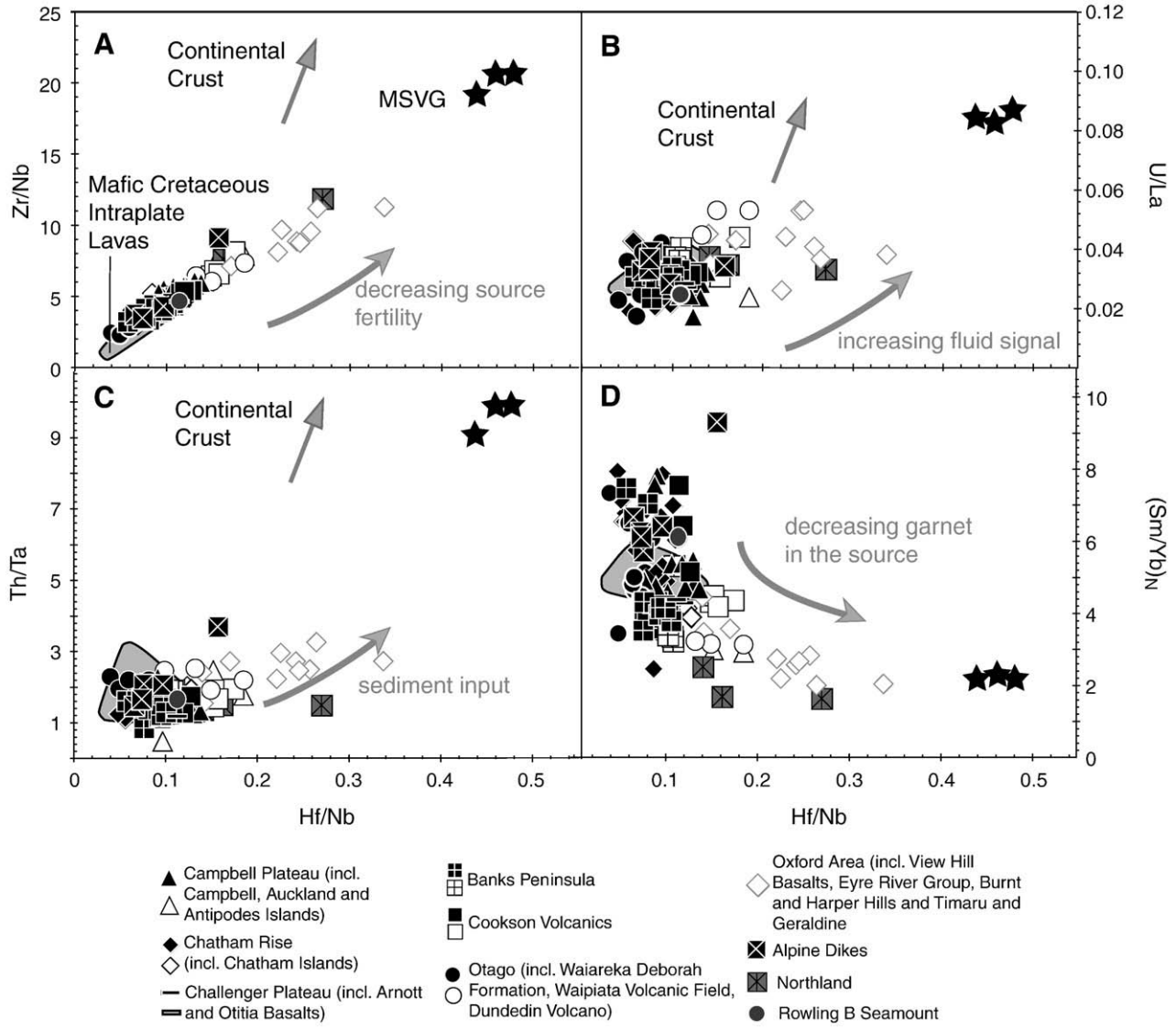

Fig. 12. Hf/Nb versus (A) Zr/Nb, (B) U/La, (C) Th/Ta and (D) $(Sm/Yb)_N$ (n = normalized to primitive mantle) of mafic (MgO>5 wt.%) Cenozoic Zealandia intraplate lavas illustrate that the high-silica group are likely to have undergone greater amounts of lithospheric contamination (or at least show greater amounts of lithospheric contamination due to their originally lower incompatible-element abundances) than the low-silica group lavas and that the low-silica group overlaps largely in composition with the Cretaceous intraplate volcanic rocks on Zealandia. The Cretaceous subduction-related lavas of the Mount Somers Volcanic Group (data are taken from Tappenden, 2003 and Mortimer et al., 2006) serve as a possible endmember for assessing the composition of the lithosphere enriched by subduction, when Zealandia formed part of the Gondwana margin. The increasing imprint of a subduction component from lithospheric interaction or direct melting of the lithosphere on the asthenospheric intraplate melts is indicated by decreasing Nb, whereas Zr and Hf remain relatively unchanged, resulting in an increase in Zr/Nb and Hf/Nb ratios. Increasing sediment (subducted or within the crust) and fluid contributions in some lavas is indicated by increasing Th/Ta (increasing Th together with decreasing Ta) and U/La ratios. Decreasing $(Sm/Yb)_N$ reflects decreasing quantities of garnet in the source. Increasing Hf/Nb combined with decreasing $(Sm/Yb)_N$ reflects a change from an OIB-type to a more subduction-related source.

enriched by subduction, when Zealandia formed part of the Gondwana margin. Although the variations in the isotopic composition of the Banks Peninsula rocks could be explained by assimilation of crustal rocks (Mt. Somers and/or Torlesse sediments), the major and trace element compositions of the mafic high-silica rocks from Banks Peninsula could not be modeled simply through mixing/assimilation of crustal rocks by low-silica HIMU-type melts, suggesting that the lithospheric mantle also plays a role in imparting the "enriched" signature on the intra-plate rocks (Timm et al., 2009). The crustal rocks with appropriate endmember compositions (e.g. Mt. Somers volcanic rocks and Torlesse Group sediments) are related to Mesozoic subduction along the Gondwana margin. The melts forming the volcanic rocks passed directly through the lithospheric mantle and no doubt would have also metasomatized the lithospheric mantle on their way to the surface or stagnated and crystallized directly within the lithospheric mantle, imparting their isotopic and highly incompatible-element ratios on the lithospheric mantle. The Torlesse sediments, on the other hand, are largely derived from subduction-related volcanic rocks that passed through the lithospheric mantle.

The Mt. Somers lavas have incompatible-element ratios characteristic of subduction-zone volcanic rocks (e.g. Fig. 12). High Th/Ta and U/(La, Nb) are indicative of source enrichment by hydrous fluids/melts from subducted altered oceanic crust and marine sediments, while high (Zr, Hf, La)/Nb ratios reflect Nb (HFSE) depletion relative to other highly to moderately incompatible (e.g. LILE) elements in the melts. Low $(Sm/Yb)_N$, on the other hand, reflect lower amounts of garnet in the source. On incompatible-element ratio diagrams, the Cenozoic high-silica rocks trend from the field of the low-silica rocks towards the Mt. Somers volcanic rock field, suggesting greater amounts of interaction of these magmas with lithosphere (crust and/or mantle) affected by Gondwana subduction than for the low-silica rocks (Hoernle et al., 2006; Timm et al., 2009).

Please cite this article as: Timm, C., et al., Temporal and geochemical evolution of the Cenozoic intraplate volcanism of Zealandia, Earth-Science Reviews (2009), doi:10.1016/j.earscirev.2009.10.002

In summary, the high-silica volcanic rocks from Zealandia can be grouped into high- and low-iron groups. The low-iron melts were formed at the lowest pressures (average depths of ~35–50 km) and temperatures (~1250–1400 °C) of an E-MORB-type peridotitic mantle. The high-iron, high-silica group melts instead are generated at higher pressures (at depth between ~65 and 100 km) and temperatures (~1350–1500 °C) and experienced extensive interaction with (or are derived directly from) the EMII-type lithosphere (mantle and crust), enriched by prior subduction.

5.6. Evaluation of previously proposed models for the origin of the Cenozoic intraplate volcanism on Zealandia

The new $^{40}Ar/^{39}Ar$ age data clearly contradict the crude WNW to ESE age progression in volcanism postulated by Adams (1981) and show that there is considerably more overlap between the age ranges of the individual volcanic fields than previously recognized (Fig. 4). This, as well as the longevity of the Cenozoic volcanism, argues against an origin involving relative movement of Zealandia over a linear mantle region of upwelling asthenosphere as proposed by Adams (1981) or Farrar and Dixon (1984).

Another conceivable source of the HIMU-type component in the Cenozoic magmas is a plume swarm. The occurrence of volcanism in a very restricted region on the Chatham Rise, Marlborough, Otago and in Canterbury for more than 60 million years on a fast-moving plate (~60 mm/year) is, however, incompatible with the classic hotspot hypothesis (Hoernle et al., 2006), which should generate chains of volcanoes that become progressively older in the direction of plate motion (Figs. 2, 4, 9 and 13). Although the classic model is for hotspots fixed relative to plate motions, it has been shown that mantle plumes are not necessarily stationary and can move large distances over tens of millions of years. The Hawaiian plume, for example, moved more than 1000 km over ~40 million years (Tarduno et al., 2003; Steinberger et al., 2004). Multiple plumes that moved more than ~4000 km with the Zealandia micro-continent since ~60 Ma, however, would be required beneath the fast-moving Zealandia micro-continent, as well as beneath an essentially stationary West Antarctica, which does not appear to be feasible based on our present knowledge of plume motions. Alternatively there could be tens or hundreds of small plumelets located beneath the region over which Zealandia has passed (~4000 km) since the Cretaceous. There is, however, no seismic evidence for widespread shallow thermal anomalies (low S and P wave velocities) (Finn et al., 2005; Priestley and McKenzie, 2006, Montelli, et al., 2006, Nolet et al., 2006 and Li et al., 2008) beneath Zealandia.

Although volcanic rocks with intraplate geochemical characteristics can be generated in areas of continental rifting and extensional tectonics, major continental rifting between Zealandia and Antarctica ceased in the Late Cretaceous. Localized extensional tectonic events on Zealandia may have facilitated the rise of some magmas to the

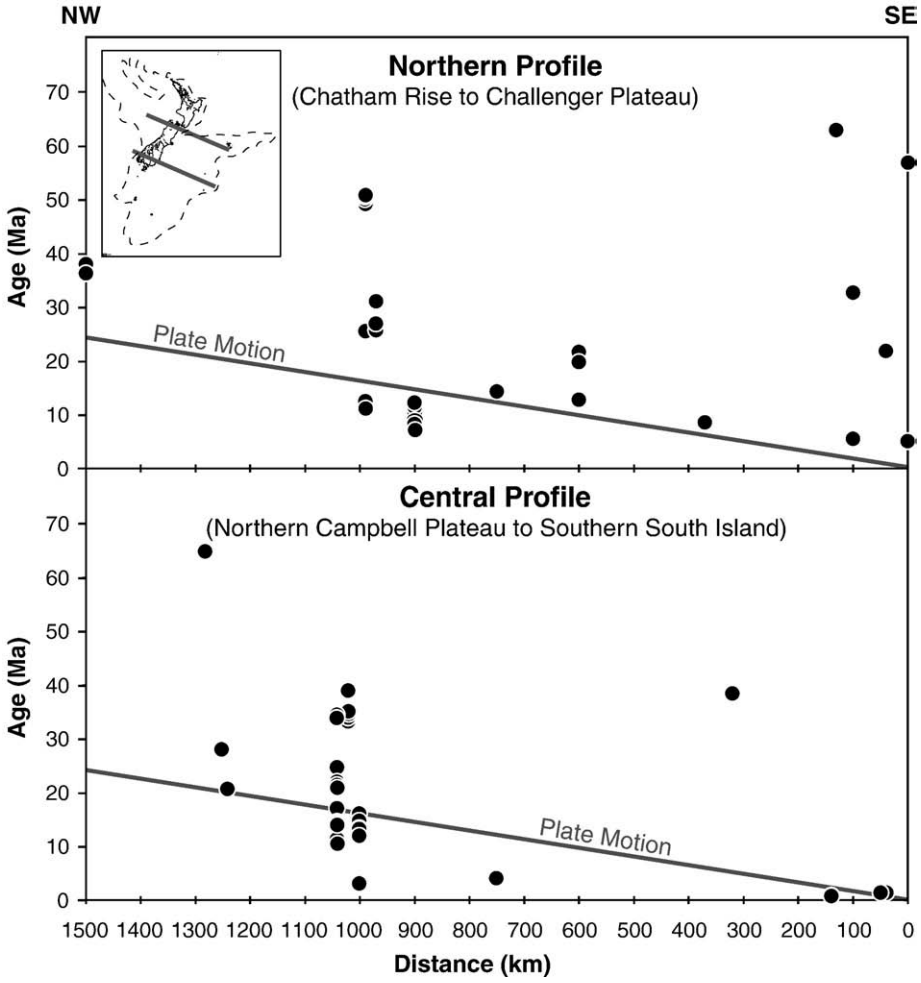

Fig. 13. Ages of volcanism have been projected onto two profiles in the direction of plate motion (after Clouard and Bonneville, 2005) in the inset, demonstrating that there are no systematic age progressions in the direction of plate motion on the northern and central parts of Zealandia. The lines on the distance versus age diagrams represent possible age-progressive trends, assuming current plate velocity of 6.1 cm/yr (see Fig. 1 for ages). The lines representing possible age progressions can be moved up or down vertically (as long as the slope of the lines aren't changed), but still no clear age progressions are observed, because volcanism occurred episodically at individual locations throughout the Cenozoic.

Please cite this article as: Timm, C., et al., Temporal and geochemical evolution of the Cenozoic intraplate volcanism of Zealandia, Earth-Science Reviews (2009), doi:10.1016/j.earscirev.2009.10.002

surface and may even be responsible for generating some low-level volcanic activity (Weaver and Smith, 1989), for example isolated monogenetic volcanoes or even volcanic fields. Nevertheless, OIB-type volcanism occurred in Zealandia both in times of extension (Cretaceous), passive drift (Paleogene) and compression (Neogene) and it is difficult to explain large volumes of, for example, composite shield volcanism through localized extensional events. Moreover, our new age data suggest that the intensity of intraplate volcanism on Zealandia may have even increased during the period of compressional tectonics (i.e. since ~22 Ma; Cooper et al., 1987; Cooper and Paterson, 2008; see Fig. 4), excluding major extensional tectonics as the controlling factor in generating Cenozoic intraplate volcanism on Zealandia.

Finn et al. (2005) proposed that catastrophic slab detachment along the Gondwana margin in the Late Cretaceous induced upward mantle flow in a broad region of the upper asthenosphere to the base of the metasomatized lower subcontinental lithosphere beneath Zealandia, Australia and Antarctica, with the increased temperature causing partial melting in the base of the lithosphere. The mixing of metasomatized subcontinental lithospheric mantle with warm Pacific asthenosphere explains the diversity of mantle sources (HIMU, EM and MORB) of a huge diffuse alkaline magmatic province (DAMP) now dispersed on both sides of the Tasman Sea and Southern Ocean. Although we agree that the EM component may be located in the lithospheric mantle metasomatized by subduction-zone fluids and sediment melts, we do not agree that volcanism associated with the formation of the composite shield volcanoes can be derived solely from conductive melting of the base of the lithospheric mantle beneath Zealandia in absence of lithospheric removal. Furthermore, a universal characteristic of subduction-zone volcanism (excluding minor backarc volcanism) is trace element signatures characterized by relative depletions in Nb and Ta and the lack of relative depletion or enrichment in Pb; this signature is found in the Cretaceous Gondwana subduction lavas, for example in the Mount Somers volcanic group (Tappenden, 2003; Mortimer et al., 2006). Subduction-zone trace element signatures also show large enrichments in fluid-mobile elements versus fluid-immobile elements. None of these characteristics is observed in the silica-undersaturated Cenozoic basalts from Zealandia and we therefore rule out derivation of the Cenozoic basanites and some alkali basalts from subduction-modified lithospheric mantle.

Coombs et al. (1986) noted the similarity in Sr and Nd isotopic composition of Cenozoic basalts on the South Island of New Zealand to 1) volcanic rocks from St. Helena and Tubuai (type localities for the HIMU component in ocean island basalts) and 2) basalts from Marie Byrd Land, Antarctica and Australia. They point out that the areas having volcanism with HIMU-type Sr and Nd isotopic compositions on these three continental blocks were contiguous prior to 100 Ma but rifted apart at c. 80 Ma, suggesting that this volcanism was derived from a common, probably lithospheric, source. Later authors have expanded on this idea proposing that a fossil HIMU plume head, involved in the last breakup phase of Gondwana (Weaver et al., 1994; Storey et al., 1999), is located at the base of the lithosphere beneath these formerly connected areas (Hart et al., 1997; Panter et al., 2000; Panter et al., 2006).

Panter et al. (2006) and Sprung et al. (2007) suggest that different mixing proportions of a degassed upper asthenosphere having a MORB-like composition with HIMU-signature melts that metasomatized the lower MORB-like lithospheric mantle, can melt to generate the isotopic compositions of the Cenozoic lavas. Although we cannot preclude a HIMU-domain residing in the lithospheric mantle, it remains unclear, however, why some of the same lithospheric domains would repeatedly melt throughout the Cenozoic. We also again note that it may be possible to explain some of the low-level (monogenetic) volcanism through lithospheric melting as a result of conductive heating from the asthenosphere but not the larger (>100 km^3) events, in particular the formation of composite shield volcanoes, such as the Akaroa Volcano, with volumes of up to 1200 km^3 that largely formed within 1–2 Ma (Timm et al., 2009).

A number of studies have investigated the process of delaminating dense lower lithosphere (e.g. Conrad and Molnar, 1997; Houseman and Molnar, 1997; Neil and Houseman, 1999; Jull and Kelemen, 2001), which may, for example, have caused the formation of the Transverse Ranges in Colorado (Houseman et al., 2000) and Cenozoic intraplate basalt volcanism in Mongolia (Barry et al., 2003). Lithospheric detachment has also been proposed to explain minor younger (at ~90 Ma) volcanism on the Ontong Java Plateau (Korenaga, 2005). In accordance with this model, detachment of dense lithosphere, containing eclogite, garnet pyroxenite and Fe-rich garnet-lherzolite, beneath the plateau drives convective currents, which can possibly even cause detached mantle to upwell locally and melt. Lithospheric removal (detachment) has been proposed as an alternative model for triggering Cenozoic partial melting beneath Zealandia (Hoernle et al., 2006; Timm et al., 2009). Prolonged exposure to the passage of subduction-related and possibly also plume-related magmas during the Mesozoic fertilized the lower lithospheric mantle, increased its density with respect to the underlying asthenospheric mantle and thereby produced a negatively buoyant, gravitationally unstable layer. In response to the sinking of domains of dense lower lithosphere, less-dense upper asthenosphere streams up and partially melts by decompression. The HIMU-type component was linked to the presence of pyroxenite/eclogite in a depleted peridotitic matrix within the upper asthenospheric mantle.

5.7. Towards an integrated model to explain the Cenozoic intraplate volcanism on Zealandia

In the Cenozoic, Zealandia drifted ~4000 km to the north/northwest, but low-volume intraplate volcanism was widespread over the entire micro-continent. As discussed above, there is no evidence for belts of age-progressive volcanism or seismic evidence for shallow low-velocity anomalies beneath Zealandia, which would be expected if fixed plumes were involved in generating this intraplate volcanism (Finn et al., 2005; Priestley and McKenzie, 2006). There is also little evidence for major lithospheric extension and thinning during the Cenozoic on the different parts of Zealandia. Local minor extensional events, or lithospheric melting due to heat conduction from the asthenosphere, is also not sufficient to generate the extensive partial melting necessary to account for the amount of magma required to form composite shield volcanoes. Due to the problems with other models discussed above, we favor local lithospheric removal as the major (but not necessarily exclusive) trigger for causing partial melting beneath Zealandia: primarily through decompression melting of the upper asthenosphere upwelling into the void left by removal of parts of the base of the lithosphere combined with some lithospheric melting. In order to explain the HIMU-type composition of the basalts, Hoernle et al. (2006) and Timm et al. (2009) proposed that young (between ~0.9 and 1.3 Ga) recycled oceanic crust/lithosphere in the form of eclogite/pyroxenite was present in the upper asthenosphere. We note, however, that this interpretation does not explain why the Sr–Nd–Pb–Hf isotopic composition of the Cenozoic low-silica intraplate volcanism forms arrays extending from the field of the Cretaceous intraplate volcanism to MORB, which implies that the Cenozoic volcanism could be derived by mixing of the Cretaceous volcanic source with the depleted upper mantle.

As noted above, large volumes of Cretaceous (99–89 Ma) HIMU-type volcanism have been found on the Hikurangi Plateau (Hoernle et al., 2005) and minor volcanic activity occurred on the South Island of New Zealand (e.g. Tapuaenuku Igneous Complex, Baker et al., 1994; Mandamus intrusive and extrusive rocks, Tappenden, 2003). The Cretaceous HIMU-type volcanism on the Hikurangi Plateau may give

Please cite this article as: Timm, C., et al., Temporal and geochemical evolution of the Cenozoic intraplate volcanism of Zealandia, Earth-Science Reviews (2009), doi:10.1016/j.earscirev.2009.10.002

us the best idea about the composition of the Cretaceous plume head, since they erupted through oceanic lithosphere on the incoming plate and therefore avoided interaction with the Gondwana mantle wedge and continental lithosphere. Nevertheless, the composition of the Cretaceous volcanic rocks from the Tapuaenuku and Mandamus Igneous Complexes are similar to the Hikurangi lavas, although they were emplaced inboard the former subduction. Both P- and S-wave seismic tomographic studies show that a large-scale, deep-seated low-velocity zone is present between depths of ~600–1450 km, extending from beneath the Chatham Rise to beneath western Antarctica margin, shallowing to ~300 km beneath some areas (Montelli et al., 2006; Nolet et al., 2006; Li et al., 2008). If this tomographic anomaly represents the source of the Cretaceous volcanism, we speculate that it may have extensively polluted the uppermost asthenosphere with HIMU-type material, variably enriched in an eclogitic component derived from recycled ancient ocean crust (Fig. 14). As a result the uppermost asthenosphere could reflect a mixture of HIMU-type eclogitic and depleted MORB-source-type peridotitic mantle. Our conclusion is supported by a study of $^{3}He/^{4}He$ isotope ratios on fluid inclusions in mantle xenocrysts and basalt phenocrysts from the South Island, which point to a more degassed upper MORB-like mantle source beneath Zealandia, containing remnants of plume material (Hoke et al., 2000). Although not many Cenozoic oceanic basalts have been analyzed between Zealandia and Antarctica, available isotope data from Balleny and Scott Island (Hart et al., 1997; Panter et al., 2000) also show HIMU-like signatures ($^{206}Pb/^{204}Pb > 19.5$), suggesting a large-scale reservoir for the HIMU-type mantle consistent with the large-scale seismic tomographic anomaly.

Subduction throughout the Mesozoic along the Gondwana margin may have overprinted the Zealandia lithosphere not only with an EM-type geochemical signature, but also with subduction-related melts that froze in the lower lithosphere forming eclogite and ultramafic cumulates, e.g. garnet pyroxenite. These dense rocks would have significantly increased the density of the lowermost lithosphere (Elkins-Tanton, 2007), pre-conditioning it for later lithospheric

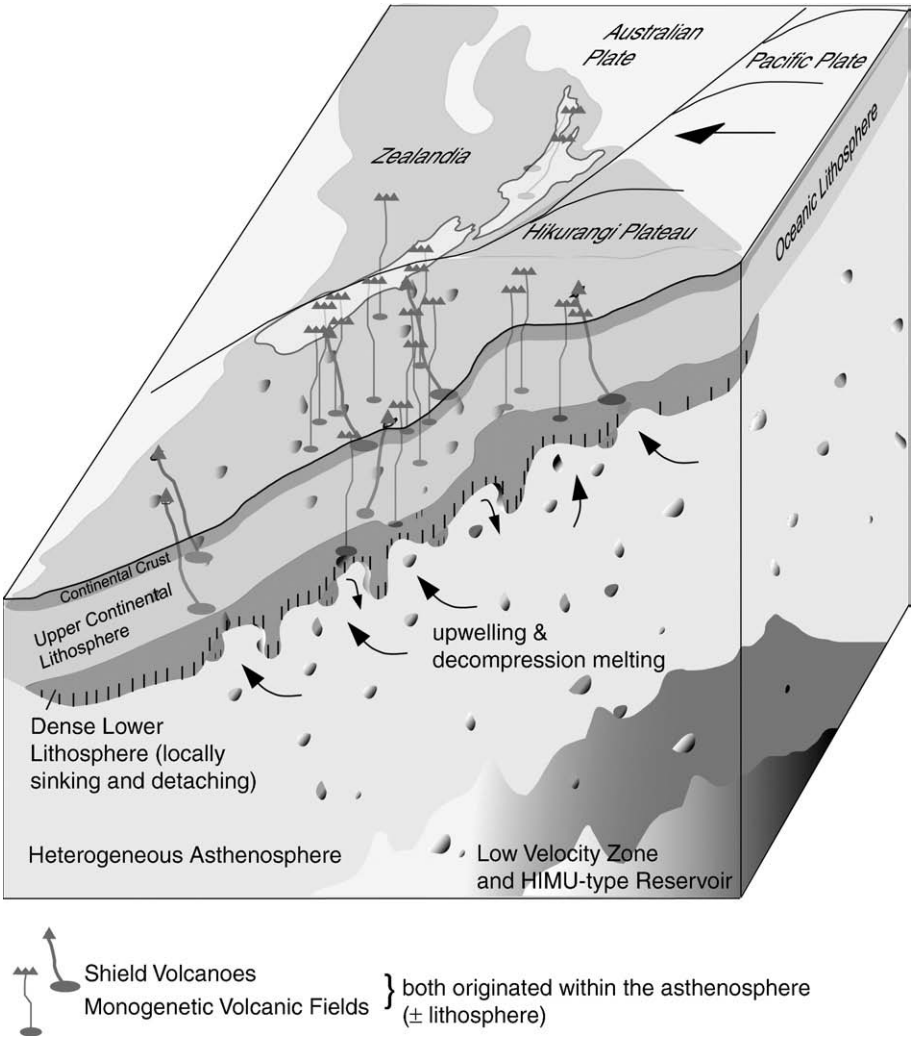

Fig. 14. Schematic box model to explain melt generation beneath Zealandia. A large-scale hot thermal anomaly was identified beneath the Chatham Rise by seismic tomography at ~600 km depth (P- and S-waves) (Montelli et al., 2006; Nolet et al., 2006; Li et al., 2008). If this thermal anomaly represents the source of Cretaceous HIMU-plume-type volcanic rocks, it could pollute the upper asthenosphere with carbonated eclogitic (recycled ancient ocean crust) plume material with a HIMU-type composition. Based on Montelli et al. (2006) and Li et al. (2008), the velocity anomaly below ~600 km can be traced to the south all the way to western Antarctica. We invoke lithospheric removal to trigger melting, which induces upwelling of asthenospheric mantle and partial melting of carbonated eclogite within depleted upper asthenospheric peridotite. The mixing proportion between eclogite and peridotite melts controls the extent of the HIMU-type signature found in the Cenozoic lavas erupted on Zealandia. The extent of melting is controlled by the extent of lithospheric detachment, which in turn controls the degree of upwelling and the amount of decompression melting. Low-silica melts are formed by low degrees of melting primarily sampling carbonated eclogite, while larger degrees of melting preferentially sample depleted peridotite producing high-silica melts with MORB-type compositions. The depleted high-silica melts are preferentially contaminated in the lithospheric mantle that has enriched (EMII-type) incompatible element and isotope ratios inherited from Gondwana subduction. Melting of metasomatized, volatile-rich portions of the detached/delaminated lithospheric mantle (containing amphibole/phlogopite or carbonated eclogite) could also contribute to the formation of both HIMU- and EMII-type melts.

Please cite this article as: Timm, C., et al., Temporal and geochemical evolution of the Cenozoic intraplate volcanism of Zealandia, Earth-Science Reviews (2009), doi:10.1016/j.earscirev.2009.10.002

detachment in response to continental extension and break-up at the end of the Cretaceous. As Zealandia drifted northwards, repeated but more localized detachment of parts of the dense lithospheric root led to localized upwelling, melting and volcanism. Small-scale detachment events could generate minor upwelling and low-degree melting, preferably of eclogite to form low-silica magmas (Hoernle et al., 2006). If these events occurred repeatedly or re-occurred regularly at the same locations on the moving continental mass, low levels of volcanism could be maintained over long periods of time in the same area. On the other hand, detachment of larger bodies, or a rapid succession of small detachment events, could generate more extensive upwelling and melting to form shield volcanoes within short time scales of 1–4 Ma. More extensive melting of the upwelling asthenosphere would exhaust the eclogitic component, resulting in primarily melting of depleted peridotitic upper mantle. These melts have higher silica and more depleted (E-MORB-type) compositions. More extensive melting would also result in the greater transfer of heat to the lithosphere by larger volumes of ascending melts, causing areas enriched during Gondwana subduction to melt, resulting in larger amounts of lithospheric interaction. Greater lithospheric interaction with the more depleted (low in incompatible-element abundances), larger-degree, largely (E-MORB-type) peridotitic melts would result in more noticeable contamination by subduction-related EM-type components in the lithosphere (both mantle and crust). Peridotitic melts, for example in Northland, that have depleted (E-MORB-type) isotopic compositions could have ascended through areas of thinner lithosphere and possibly through lithosphere that was not as extensively affected by Gondwana subduction, arriving at the surface with minimal interaction with enriched lithosphere. This model explains both the depleted (E-MORB)- and enriched (EM)-type compositions of the high-silica melts.

During Gondwana subduction, the lithosphere was enriched by subduction-zone melts with EM-type compositions, whereas the lithosphere could have been enriched by HIMU-type melts in the mid-Cretaceous during the formation of the Tapuaenuku and Mandamus igneous complexes. Melting and recycling of detached lower lithosphere could therefore also be the source of both low-silica HIMU-type and the high-silica EMII-type melts. Detached lithospheric mantle, enriched by Cretaceous HIMU-type melts, could melt after removal from the base of the lithosphere and these melts could mix with depleted upper MORB-source-type mantle or melts derived from such mantle to form the low-silica HIMU-type melts. Unequivocal evidence for the presence of residual amphibole or phlogopite in the source of the low-silica HIMU-type melts (e.g. Class and Goldstein, 1997) could provide evidence that at least some of the low-silica melts are derived from lithospheric sources (e.g. Panter et al., 2006). It is difficult, however, to distinguish if low-silica melts derived from eclogite come from the asthenosphere or from detached lithosphere, or possibly both. Sinking of volatile-rich mantle (containing amphibole and/or phlogopite or carbonated eclogite) into the upper asthenosphere could trigger melting of large amounts of lithosphere in a geologically short time period to produce more extensive volcanism. After removal of lithosphere with HIMU-type composition (containing either amphibole/phlogopite and/or carbonated eclogite), pieces of the detached lithosphere could be entrained into the asthenosphere upwelling to refill the voids left by the detachment process. The HIMU-type lithosphere would be heated conductively by the hotter asthenospheric mantle and could also melt by decompression contributing to the formation of the low-silica group volcanic rocks. Volatile-release due to the breakdown of volatile-bearing phases during lithospheric detachment could also trigger lithospheric melting. The EMII-type melts could also be derived from melting detached lithosphere enriched by subduction-derived melts during Gondwana subduction, in addition to reflecting contamination of asthenospheric melts as they ascend through the lithosphere. In conclusion, the local lithospheric detachment model provides a powerful mechanism for generating relatively large volumes of melt (enough to form shield volcanoes) within relatively short time periods (1–4 Ma). This model also has the advantage that it can accommodate melting of lithospheric and asthenospheric components.

In summary, we propose that the Cenozoic volcanic rocks can be explained by mixing of sources for Cretaceous intraplate volcanism (interpreted to result from the interaction of a HIMU plume with the Gondwana mantle wedge and lithosphere) and MORB. A deep-seated, large-scale low-velocity zone, located at 650–1450 km (Fig. 14) and presumably associated with the Cretaceous volcanism, could have polluted the depleted upper MORB-source peridotitic asthenosphere with carbonated eclogite (recycled oceanic crust), having HIMU-type trace element and isotopic compositions. Low-degree, decompression melting of the primarily carbonated eclogite (representing recycled ancient ocean crust/lithosphere) during upwelling possibly metasomatized the surrounding depleted asthenosphere. Partial melting of the eclogitic component and/or of the metasomatized peridotite produces low-silica melts with primarily HIMU-type trace element and isotopic compositions. At greater degrees of decompression melting, the eclogitic component in the melts decrease, the peridotitic component increases and or the metasomatized peridotite becomes progressively depleted resulting in the generation of high-silica melts with depleted (E-MORB-type) trace element and isotopic compositions. Contamination within portions of the lithosphere, enriched during subduction along the Gondwana margin and by non-volcanic crustal rocks, primarily affects the composition of the depleted high-silica melts, due to their low incompatible-element contents. Melting of metasomatized (through subduction or older intraplate magmatism), volatile-rich detached lithosphere, containing amphibole and/or phlogopite or carbonated eclogite, could also contribute to the generation of HIMU- and EMII-type magmas.

6. Conclusions

1) Cenozoic intraplate volcanism is widespread on both the presently emergent and submerged parts of Zealandia, and occurred throughout much of the Cenozoic. No age progressions in the direction and at the rate of plate motion or close correlation with local extensional events are observed, confirming that the plume hypothesis and continental rifting/extension are not adequate models for explaining the origin of Cenozoic intraplate volcanism on Zealandia.
2) The geochemical data confirm that three different types of mantle source components are required to explain the composition of the Cenozoic volcanism on Zealandia: 1) HIMU-like component (characterized by $^{206}Pb/^{204}Pb = 19.2–20.6$) that dominates in mafic low-silica ($SiO_2 < 46$ wt.%) volcanic rocks, 2) depleted (E-MORB-type) component (characterized by $^{206}Pb/^{204}Pb = 18.6–19.0$ and $^{143}Nd/^{144}Nd = 0.51279–0.51293$) that dominates in low-iron, high-silica ($SiO_2 \geq 46$ wt.%) volcanic rocks from Northland, and 3) enriched (EMII-type) component (characterized by $^{206}Pb/^{204}Pb = 18.9–19.6$ and $^{143}Nd/^{144}Nd = 0.51296–0.51308$) that dominates in high-iron, high-silica rocks. Although the presence of a depleted (E-MORB-type) component was previously postulated, it was not previously identified.
3) The process of local lithospheric removal and subsequent decompression melting of upwelling heterogeneous asthenospheric mantle (±detached lithosphere) can best explain the distribution, ages and geochemical composition of Cenozoic intraplate volcanism across Zealandia. As proposed by Hoernle et al. (2006) and Timm et al. (2009), the heterogeneous asthenospheric mantle is likely to consist of eclogite/pyroxenite domains with HIMU-type isotopic composition within a depleted (MORB-type) peridotitic matrix. Melting of peridotite matrix metasomatized by eclogite/pyroxenite and/or detached volatile-enriched lithosphere could generate the HIMU-type low-silica melts. Melting of upwelling peridotite, not as extensively

Please cite this article as: Timm, C., et al., Temporal and geochemical evolution of the Cenozoic intraplate volcanism of Zealandia, Earth-Science Reviews (2009), doi:10.1016/j.earscirev.2009.10.002

metasomatized by melts from carbonated eclogite/pyroxenite could generate the E-MORB-type low-iron, high-silica lavas. Interaction of depleted high-silica melts with the lithosphere, enriched (both mantle and crustal parts) to various degrees by a subduction-related component as represented by the Late Cretaceous Mt. Somers volcanic rocks and/or Zealandia crust could generate the EMII-type signatures of most of the high-silica rocks. Alternatively melting of enriched detached lithosphere could also produce the EMII-type high-silica rocks.

Acknowledgements

Dagmar Rau, Jan Fietzke and Silke Hauff are thanked for their technical assistance with the major element and isotopic analyses. We are grateful to K. Gohl, chief scientist of cruise SO 169, and the SO168 and SO169 captains, crews and shipboard scientists for their expert support. B. Davy and R. Herzer provided a variety of maps, data and other invaluable information for the marine sampling. We are especially grateful to D. Coombs, T. Reay, D. Lee and A. Cooper from Otago University, H. Campbell from the GNS in Dunedin and S. Weaver and V. Tappenden from Canterbury University in Christchurch for providing us samples out of the OU, P and UC catalogues and/or for helpful advice and enlightening discussions. M. Großman and M. Thorman helped with processing of the SIMRAD data. K. Heydolph and M. Rehder are thanked for sample preparation and S. Duggen for stimulating discussions. We also thank Kurt Panter and an anonymous reviewer for constructive and helpful reviews. The German Ministry of Education and Research (BMBF; grants SO168 Zealandia and SO169 CAMP) and the DFG (grants HO18/12-1 and 2) and IFM-GEOMAR are gratefully acknowledged for providing funding for this project. Several figures were prepared with GMT public domain software (Wessel and Smith, 1995).

Appendix A. Supplementary data

Supplementary data associated with this article can be found, in the online version, at doi:10.1016/j.earscirev.2009.10.002.

References

Adam, C.J., 1980. New K/Ar age data for South Island lamprophyre dyke swarms in the Buller-S. Westland and Haast-Wanaka areas. Geological Society of New Zealand Conference, Christchurch, Nov. 24–27, Programme and abstracts, vol. 14.
Adams, C.J., 1981. Migration of late Cenozoic volcanism in the South Island of New Zealand and the Campbell Plateau. Nature 294, 153–155.
Adams, C.J., 1983. Age of the volcanoes and granite basement of the Auckland Islands, Southwest Pacific. New Zealand Journal of Geology and Geophysics 26, 227–237.
Adams, C.J., Cooper, A.F., 1996. K–Ar age of a lamprophyre dike swarm near Lake Wanaka, west Otago, South Island, New Zealand. New Zealand Journal of Geology and Geophysics 39, 17–23.
Adams, C.J., Morris, P.A., Beggs, J.M., 1979. Age and correlation of volcanic rocks of Campbell Island and metamorphic basement of the Campbell Plateau, southwest Pacific. New Zealand Journal of Geology and Geophysics 22, 679–691.
Baker, J., Gamble, J.A., Graham, I.J., 1994. The age, geology, and geochemistry of the Tapuaenuku Igneous Complex, Marlborough, New Zealand. New Zealand Journal of Geology and Geophysics 37, 249–268.
Barley, M.E., Weaver, S.D., 1988. Strontium isotope composition and geochronology of intermediate-silicic volcanics, Mt Somers and Banks Peninsula, New Zealand. New Zealand Journal of Geology and Geophysics 31, 197–206.
Barreiro, B.A., Cooper, A.F., 1987. A Sr, Nd, and Pb isotope study of alkaline lamprophyres and related rocks from Westland and Otago, South Island, New Zealand. Geological Society of America Special Paper 215, 115–125.
Barry, T.L., Saunders, A.D., Kempton, J.D., Windley, B.F., Pringle, M.S., Dorjnamjaa, D., Saandar, S., 2003. Petrogenesis of Cenozoic basalts from Mongolia: evidence for the role of asthenosphere versus metasomatized lithospheric mantle sources. Journal of Petrology 44 (1), 55–91.
Blichert-Toft, J., Albarede, F., 1997. The Lu–Hf isotope geochemistry of chondrites and the evolution of the mantle–crust system. Earth and Planetary Science Letters 148, 243–258.
Briggs, R.M., Okada, T., Itaya, T., Shibuya, H., Smith, I.E.M., 1994. K–Ar ages, paleomagnetism, and geochemistry of the South Auckland volcanic field, North Island, New Zealand. New Zealand Journal of Geology and Geophysics 37, 143–153.
Carey, C., Mortimer, N., Uruski, C., Wood, R., 1991. Fire and brimstone on the western Challenger Plateau: further evidence from Mount Spong and Megabrick. New Zealand Geological Survey Record 43, 123–128.
Class, C., Goldstein, S.L., 1997. Plume–lithosphere interactions in the ocean basins: constraints from the source mineralogy. Earth and Planetary Science Letters 150, 245–260.
Clouard, V., Bonneville, A., 2005. Ages of seamounts, islands and plateaus and plateaus on the Pacific plate. In: Foulger, G.R., Natland, J.H., Presnall, D.C., Anderson, D.L. (Eds.), Plates, Plumes, and Paradigms. Geological Society of America Special Paper: Geological Society of America, vol. 388, pp. 71–90.
Conrad, C.P., Molnar, P., 1997. The growth of Rayleigh–Taylor-type instabilities in the lithosphere for various rheological and density structures. Geophysical Journal International 129, 95–112.
Cook, C., Briggs, R.M., Smith, I.E.M., Maas, R., 2004. Petrology and geochemistry of intraplate basalts in the South Auckland Volcanic Field, New Zealand: evidence for two coeval magma suites from distinct sources. Journal of Petrology 46, 473–503.
Coombs, D.S., Cas, R.A., Kawachi, Y., Landis, C.A., McDonough, W.M., Reay, A., 1986. In: Smith, I.E.M. (Ed.), Cenozoic volcanism in North, East and Central Otago. Cenozoic Volcanism in New Zealand: Royal Society of New Zealand Bulletin, 23, pp. 278–312.
Coombs, D.S., Adams, C.J., Roser, B.P., Reay, A., 2008. Geochronology and geochemistry of the Dunedin Volcanic Group, eastern Otago, New Zealand. New Zealand Journal of Geology and Geophysics 51, 195–218.
Cooper, A.F., 1986. A carbonatitic lamprophyre dike swarm from the Southern Alps, Otago and Westland. Late Cenozoic Volcanism in New Zealand. I. E. M. Smith. Royal Society of New Zealand — Bulletin 23, 313–336.
Cooper, A.F., Paterson, L.A., 2008. Carbonatites from a lamprophyric dyke swarm, South Westland, New Zealand. Canadian Mineralogist 46, 753–777. doi:10.3749/canmin.46.4.753.
Cooper, A.F., Barreiro, B.A., Kimbrough, D.L., Mattinson, J.M., 1987. Lamprophyre dike intrusion and the age of the Alpine fault, New Zealand. Geology 15, 941–944.
Cullen, D.J., 1969. Quaternary volcanism at the Antipodes Islands: its bearing on the structural interpretation of the southwest Pacific. Journal of Geophysical Research 74, 4213–4220.
Dasgupta, R., Hirschmann, M.M., Stalker, K., 2006. Immiscible transition from carbonate-rich to silicate-rich melts in the 3 GPa melting interval of eclogite + CO3 and genesis of silica-undersaturated ocean island lavas. Journal of Petrology 47 (4), 647–671.
Dasgupta, R., Hirschmann, M.M., Smith, N.D., 2007. Partial melting experiments of peridotite + CO2 at 3 GPa and genesis of alkalic ocean island basalts. Journal of Petrology 48 (11), 2093–2124.
Davy, B., Wood, R., 1994. Gravity and magnetic modelling of the Hikurangi Plateau. Marine Geology 118, 139–151.
Davy, B., Hoernle, K., Werner, R., 2008. The Hikurangi Plateau — crustal structure, rift formation and Gondwana subduction history. Geochemistry Geophysics Geosystems 9 (7), Q07004. doi:10.1029/2007GC001855.
Duggan, M.B., Reay, A., 1986. The Timaru Basalt. Royal Society of New Zealand — Bulletin 23, 246–277.
Eagles, G., Gohl, K., Larter, R.D., 2004. High-resolution animated tectonic reconstruction of the South Pacific and West Antarctic Margin. Geochemistry Geophysics Geosystems 5 (7), 21.
Elkins-Tanton, L.T., 2007. Continental magmatism, volatile recycling, and a heterogeneous mantle caused by lithospheric gravitational instabilities. Journal of Geophysical Research 112, B03405. doi:10.1029/2005JB004072.
Farrar, E., Dixon, J.M., 1984. Overriding of the Indian–Antarctic Ridge: origin of Emerald Basin and migration of late Cenozoic volcanism in Southern New Zealand and Campbell Plateau. Tectonophysics 104, 243–256.
Finn, C.A., Mueller, R.D., Panter, K.S., 2005. A Cenozoic diffuse alkaline magmatic province (DAMP) in the southwest Pacific without rift or plume origin. Geochemistry Geophysics Geosystems 6, Q02005. doi:10.1029/2004GC000723.
Foley, S., Tiepolo, M., Vannucci, R., 2002. Growth of early continental crust controlled by melting of amphibolite in subduction zones. Nature 417, 837–840. doi:10.1038/nature00799.
Gamble, J.A., Morris, P.A., Adams, C.J., 1986. The geology, petrology and geochemistry of Cenozoic volcanic rocks from the Campbell Plateau and Chatham Rise. In: Smith, J. (Ed.), Late Cenozoic Volcanism in New Zealand. The Royal Society of New Zealand, pp. 344–365.
Garbe-Schönberg, C.-D., 1993. Simultaneous determination of thirty-seven trace elements in twenty-eight international rock standards by ICP-MS. Geostandards Newsletter 17, 81–97.
Geldmacher, J., Hanan, B.B., Blichert-Toft, J., Harpp, K., Hoernle, K., Hauff, F., Werner, R., Kerr, A.C., 2003. Hafnium isotopic variations in volcanic rocks from the Caribbean Large Igneous Province and Gala´pagos hot spot tracks. Geochemistry Geophysics Geosystems 4 (7), 1062. doi:10.1029/2002GC000477.
Godfrey, N.J., Davey, F., Stern, T., Okaya, D., 2001. Crustal structure and thermal anomalies of the Dunedin Region, South Island, New Zealand. Journal of Geophysical Research 106 (B12), 30,835–30,848.
Gohl, K., Davey, F., Davy, B., Barker, D., Uenzelmann-Neben, G., 2003. The Campbell Plateau (New Zealand) and its Rifted Margin: a history of its break-up process. Geophysical Research Abstracts 5, 2.
Grapes, R.H., Lamb, S.H., Adams, C.J., 1992. K–Ar ages of basanitic dikes, Awatere Valley, Marlborough, New Zealand. New Zealand Journal of Geology and Geophysics 35, 415–419.
Grindley, G.W., Adams, C.J., Lumb, J.T., Watters, W.A., 1977. Paleomagnetism, K–Ar dating and tectonic interpretation of upper Cretaceous and Cenozoic volcanic rocks of the Chatham Islands, New Zealand. New Zealand Journal of Geology and Geophysics 20, 425–467.
Gurenko, A.A., Sobolev, A.V., Hoernle, K.A., Hauff, F., Schmincke, H.U., 2009. Enriched, HIMU-type peridotite and depleted recycled pyroxenite in the Canary plume: a

Please cite this article as: Timm, C., et al., Temporal and geochemical evolution of the Cenozoic intraplate volcanism of Zealandia, Earth-Science Reviews (2009), doi:10.1016/j.earscirev.2009.10.002

mixed-up mantle. Earth and Planetary Science Letters 277, 514–524. doi:10.1016/j.epsl.2008.11.013.
Hart, S.R., 1984. The Dupal anomaly: a large-scale isotope anomaly in the southern hemisphere mantle. Nature 309, 753–757.
Hart, S.R., Blusztajn, J., Craddock, C., 1997. Hobbs Coast Cenozoic volcanism: implications for the West Antarctic rift system. Chemical Geology 139, 223–248.
Hémond, C., Hofmann, A.W., Vlastélic, I., Nauret, F., 2006. Origin of MORB enrichment and relative trace element compatibilities along the Mid-Atlantic Ridge between 10° and 24°N. Geochemistry Geophysics Geosystems 7 (10). doi:10.1029/2006GC001317.
Herzer, R.H., Challis, G.A., Christie, R.H.K., Scott, G.H., Watters, W.A., 1989. The Urry Knolls, late Neogene alkaline basalt extrusives, southwestern Chatham Rise. Journal of Royal Society of New Zealand 19 (2), 181–193.
Hirose, K., Kushiro, I., 1993. Partial melting of dry peridotites at high pressures: determination of compositions of melts segregated from peridotite using aggregates of diamond. Earth Planetary Science Letters 114, 477–489.
Hirschmann, M.M., Kogiso, T., Baker, M.B., Stolper, E.M., 2003. Alkalic magmas generated by partial melting of garnet pyroxenite. Geology 31, 481–484.
Hoernle, K., Tilton, G., Schmincke, H.-U., 1991. Sr–Nd–Pb isotopic evolution of Gran Canaria: evidence for shallow enriched mantle beneath the Canary Islands. Earth and Planetary Science Letters 106, 44–63.
Hoernle, K., Mortimer, N., Werner, R., Hauff, F., 2003. Fahrtbericht/Cruise Report SO 168 Zealandia (causes and effects of plume and rift-related Cretaceous and Cenozoic volcanism on Zealandia). G. R. vol. 133. 1–127+app.
Hoernle, K., Hauff, F., Werner, R., Mortimer, N., 2004. New insights into the origin and evolution of the Hikurangi oceanic plateau: Eos (Transactions, American Geophysical Union) vol. 85, pp. 401–405.
Hoernle, K., Hauff, F., Bogaard, P.van den, Werner, R., Mortimer, N., 2005. The Hikurangi oceanic plateau: another large piece of the largest volcanic event on earth. Geochim. Cosmochim. Acta Goldschmidt Conf. Abstr. vol. 69–10 Suppl. 1, p. A96.
Hoernle, K., White, J.D.L., Bogaard, P.V.D., Hauff, F., Coombs, D.S., Werner, R., Timm, C., Garbe-Schönberg, C.-D., Reay, A., Cooper, A.F., 2006. Cenozoic intraplate volcanism on New Zealand: upwelling induced by lithospheric removal. Earth and Planetary Science Letters 248, 335–352.
Hoernle, K., Abt, D.L., Fischer, K.M., Nichols, H., Hauff, F., Abers, G.A., van den Bogaard, P., Heydolph, K., Alvarado, G., Protti, M., Strauch, W., 2008. Arc-parallel flow in the mantle wedge beneath Costa Rica and Nicaragua. Nature. doi:10.1038/nature06550.
Hofmann, A.W., 1988. Chemical differentiation of the Earth: the relationship between mantle, continental and oceanic crust. Earth Planetary Science Letters 90, 297–314.
Hoke, L., Poreda, R., Reay, A., Weaver, S.D., 2000. The subcontinental mantle beneath southern New Zealand, characterised by helium isotopes in intraplate basalts and gas-rich springs. Geochimica et Cosmochimica Acta 64 (14), 2489–2507.
Houseman, G.A., Molnar, P., 1997. Gravitational (Rayleigh–Taylor) instability of a layer with non-linear viscosity and convective thinning of the continental lithosphere. Geophysical Journal International 128, 125–150.
Houseman, G.A., Neil, E., Kohler, M.D., 2000. Lithospheric instability in the traverse ranges of California. Journal of Geophysical Research 105 (B7), 16,237–16,250.
Huang, Y., Hawkesworth, C., van Calsteren, P., Smith, I., Black, P., 1997. Melt generation models for the Auckland volcanic field, New Zealand: constraints from U–Th isotopes. Earth and Planetary Science Letters 149, 67–84.
Jull, M., Kelemen, P.B., 2001. On conditions for lower crustal convective instability. Journal of Geophysical Research 106, 6423–6446.
Kogiso, T., Hirschmann, M.M., 2006. Partial melting experiments of bimineralic eclogite and the role of recycled mafic oceanic crust in the genesis of ocean island basalts. Earth and Planetary Science Letters 249, 188–199.
Korenaga, J., 2005. Why did not the Ontong Java Plateau form subaerially? Earth and Planetary Science Letters 234, 385–399.
Landis, C.A., Campbell, J., Begg, J.G., Mildenhall, D.C., Paterson, A.M., Trewick, S.A., 2008. The Waipounamu Erosion Surface: questioning the antiquity of the New Zealand land surface and terrestrial fauna and flora. Geological Magazine 145 (2), 173–197.
Larter, R.D., Cunningham, A.P., Barker, P.F., Gohl, K., Nitsche, F.O., 2002. Tectonic evolution of the Pacific margin of Antarctica 1. Late Cretaceous tectonic reconstructions. Journal of Geophysical Research 107 (B12), 19.
Le Maitre, R. W. (editor), Streckeisen, A., Zanettin, B., Le Bas, M. J., Bonin, B., Bateman, P., Bellieni, G., Dudek, A., Efremova, S., Keller, J., Lamere, J., Sabine, P. A., Schmid, R., Sörensen, H., and Woolley, A. R., Igneous rocks: a classification and glossary of terms, recommendations of the International Union of Geological Sciences, Subcommission of the Systematics of Igneous Rocks. Cambridge University Press, 2002.
Li, C., van der Hilst, R.D., Engdahl, E.R., Burdick, S., 2008. A new global model for P wave speed variations in Earth's mantle. Geochemistry Geophysics Geosystems 9 (5), Q05018. doi:10.1029/2007GC001806.
Liu, Z., Bird, P., 2006. Two-dimensional and three-dimensional finite element modelling of mantle processes beneath central South Island, New Zealand. Geophysical Journal International 365, 1003–1028.
Luyendyk, B.P., 1995. Hypothesis for Cretaceous rifting of East Gondwana caused by subducted slab capture. Geology 23, 373–376.
Mathews, W.H., Curtis, G.H., 1966. Date of the Pliocene–Pleistocene boundary in New Zealand. Nature 212, 979–980.
McDougall, I., Coombs, D.S., 1973. Potassium–Argon ages for the Dunedin Volcano and outlying volcanics. New Zealand Journal of Geology and Geophysics 16 (2), 179–188.
McLennan, J.M., Weaver, S.D., 1984. Olivine–nephelinite at Mounseys Creek, Oxford, Canterbury (Note). New Zealand Journal of Geology and Geophysics 27, 389–390.
Molnar, P., Anderson, H.J., Audoine, E., Eberhart-Phillips, D., Gledhill, K.R., Klosko, E.R., McEvilly, T.V., Okaya, D., Savage, K.M., Stern, T., Wu, F.T., 1999. Continuous deformation versus faulting through the continental lithosphere of New Zealand. Science 286, 516–519.
Montelli, R., Nolet, G., Dahlen, R.A., Masters, G., 2006. A catalogue of deep mantle plumes: new results from finite frequency tomography. Geochemistry Geophysics Geosystems 7 (11), Q11007. doi:10.1029/2006GC001248.
Morgan, W.J., 1971. Convection plumes in the lower mantle. Nature 230, 42–43.
Morris, J. C. 1987: The stratigraphy of the Amuri Limestone group, east Marlborough, New Zealand. Unpublished Ph.D. thesis, lodged in the Library, University of Canterbury. 388 pp.
Mortimer, N., 2004. New Zealand's geological foundations. Gondwana Research 7 (1), 261–272.
Mortimer, N., Hoernle, K., Hauff, F., Palin, J.M., Dunlap, W.J., Werner, R., Faure, K., 2006. New constraints on the age and evolution of the Wishbone Ridge, southwest Pacific Cretaceous microplates, and Zealandia–West Antarctica breakup. Geology 34 (3), 185–188.
Mortimer, N., Herzer, R.H., Gans, P.B., Laporte-Magoni, C., Calvert, A.T., Bosch, D., 2007. Oligocene–Miocene tectonic evolution of the South Fiji Basin and Northland Plateau, SW Pacific Ocean: evidence from petrology and dating of dredged rocks. Marine Geology 237, 1–24.
Nathan, S., Anderson, H.J., Cook, R.A., Herzer, R.H., Hoskins, R.H., Raine, J.I., Smale, D., 1986. Cretaceous and Cenozoic sedimentary basins of the West Coast Region, South Island, New Zealand. New Zealand Geological Survey Basin Studies 1, 9–18.
Neil, E., Houseman, G.A., 1999. Rayleigh–Taylor instability of the upper mantle and its role in intraplate orogeny. Geophysical Journal International 138, 89–107.
Nolet, G., Karato, S.-I., Montelli, R., 2006. Plume fluxes from seismic tomography. Earth and Planetary Science Letters 248, 685–699.
Panter, K.S., Hart, R.S., Kyle, P.R., Blusztain, J., Wilch, T., 2000. Geochemistry of Late Cenozoic basalts from the Crary Mountains: characterisation of mantle sources in Marie Byrd Land, Antarctica. Chemical Geology 165, 215–241.
Panter, K.S., Blusztain, J., Hart, R.S., Kyle, P.R., Esser, R., McIntosh, W.C., 2006. The origin of HIMU in the SW Pacific: evidence from intraplate volcanism in southern New Zealand and subantarctic islands. Journal of Petrology. doi:10.1093/petroogy/eg1024, 1–32.
Pertermann, M., Hirschmann, M.M., et al., 2004. Experimental determination of trace element partitioning between garnet and silica-rich liquid during anhydrous partial melting of MORB-like eclogite. Geochemistry Geophysics Geosystems 5 (5), Q05A01. doi:10.1029/2003GC000638.
Pfänder, J.A., Münker, C., Stracke, A., Mezker, K., 2007. Nb/Ta and Zr/Hf in ocean island basalts — implications for crust–mantle differentiation and the fate of Niobium. Earth and Planetary Science Letters 254, 158–172.
Phillips, C.J., Cooper, A.F., Palin, J.M., Nathan, S., 2005. Geochronological constraints on Cretaceous–Paleocene volcanism in South Westland. New Zealand, New Zealand Journal of Geology and Geophysics 48, 1–14.
Pilet, S., Baker, M.B., Stolper, E.M., 2008. Metasomatized lithosphere and the origin of alkaline lavas. Science 320. doi:10.1126/science.1156563.
Price, R.J., Compston, W., 1973. The geochemistry of the Dunedin volcano: strontium isotope chemistry. Contributions to Mineralogy and Petrology 42, 55–61.
Price, R.C., Cooper, A.F., Woodhead, J.D., Cartwright, I.A.N., 2003. Phonolitic diatremes within the Dunedin Volcano, South Island, New Zealand. Journal of Petrology 44, 2053–2080.
Priestley, K., McKenzie, D., 2006. The thermal structure of the lithosphere from shear wave velocities. Earth and Planetary Science Letters 244, 285–301.
Reay, A., Sipiera, P.P., 1987. Mantle xenoliths from the New Zealand region. In: Nixon, P.H. (Ed.), Mantle Xenoliths. John Wiley and Sons Ltd, pp. 347–358.
Sclater, J.G., Jaupart, C., Galson, D., 1980. The heat flow through oceanic and continental crust and the heat loss of the Earth. Reviews of Geophysics and Space Physics 18, 269–311.
Sewell, R.J., Gibson, I.L., 1988. Petrology and geochemistry of Tertiary volcanic rocks from inland Central and South Canterbury, South Island, New Zealand. New Zealand Journal of Geology and Geophysics 31, 477–492.
Sewell, R.J., Nathan, S., 1987. Geochemistry of Late Cretaceous an Early Tertiary basalts from south Westland. New Zealand Geological Survey Record 18, 87–94.
Smith, I.E.M., Okada, T., Itaya, T., Black, P.M., 1993. Age relationships and tectonic implications of late Cenozoic basaltic volcanism in Northland, New Zealand. New Zealand Journal of Geology and Geophysics 36, 385–393.
Sprung, P., Schuth, S., Münker, C., Hoke, L., 2007. Intraplate volcanism in New Zealand: the role of fossil plume material and variable lithospheric properties. Contributions Mineralogy Petrology 153, 669–687.
Steinberger, B., Sutherland, R., O'Connell, R.J., 2004. Prediction of Emperor-Hawaii seamount locations from a revised model of global plate motion and mantle flow. Nature 430, 167–173.
Stern, T., Okaya, D., Scherwath, M., 2002. Structure and strength of a continental transform from onshore–offshore seismic profiling of South Island, New Zealand. Earth Planets Space 54, 1011–1019.
Stipp, J.J., McDougall, I., 1968. Geochronology of the Banks Peninsula volcanoes, New Zealand. New Zealand Journal of Geology and Geophysics 11, 1239–1260.
Storey, B.C., 1995. The role of mantle plumes in continental breakup: case histories from Gondwanaland. Nature 377, 301–308.
Storey, B.C., Leat, P.T., Weaver, S.D., Pankhurst, R.J., Bradshaw, J.D., Kelley, S., 1999. Mantle plumes and Antarctica–New Zealand rifting: evidence from mid-Cretaceous mafic dykes. Journal of the Geological Society of London 156, 659–671.
Sun, S.-S., McDonough, W.F., 1989. Chemical and isotopic systematics of oceanic basalts: implications for mantle composition and processes. In: Saunders, A.D., Norry, M.J. (Eds.), Magmatism in the Ocean Basins, vol. 42. Geological Society, London, pp. 313–345. Special Publications.
Sutherland, R., 1995. The Australia–Pacific boundary and Cenozoic plate motions in the SW Pacific: some constraints from Geosat data. Tectonics 14 (4), 819–831.
Tappenden, V. (2003). Magmatic response to the evolving New Zealand Margin of Gondwana during the Mid-Late Cretaceous. Department of Geological Sciences Christchurch, University of Canterbury. PhD, 250.

Please cite this article as: Timm, C., et al., Temporal and geochemical evolution of the Cenozoic intraplate volcanism of Zealandia, Earth-Science Reviews (2009), doi:10.1016/j.earscirev.2009.10.002

Tarduno, J.A., Duncan, R.A., Scholl, D.W., Cottrell, R.D., Steinberger, B., Thordason, T., Kerr, B.C., Neal, C.R., Frey, F.A., Torii, M., Carvallo, C., 2003. The Emperor seamounts: southward motion of the Hawaiian hotspot plume in earth's mantle. Science 301, 1064–1069.

Timm, C., Hoernle, K., Bogaard, P.V.D., Bindemann, I., Weaver, S.D., 2009. Geochemical evolution of intraplate volcanism at Banks Peninsula, New Zealand: interaction between asthenospheric and lithospheric melts. Journal of Petrology 50 (6), 989–1023.

Todt, W., Cliff, R.A., Hanser, A., Hofmann, A.W., 1996. $^{202}Pb + ^{205}Pb$ double spike for lead isotopic analyses. In: Basu, A, Hart, S (Eds.), Earth Processes: Reading the Isotopic Code: Geophysical Monograph, vol. 95.

Turner, S., Tonarini, S., Bindeman, I., Leeman, W.P., Schaefer, B.F., 2007. Boron and oxygen isotope evidence for recycling of subducted components over the past 2.5 Gyr. Nature 447. doi:10.1038/nature05898.

Uenzelmann-Neben, G., Grobys, J., Gohl, K., Barker, D., 2009. Neogene sediment structures in Bounty Trough, eastern New Zealand: influence of magmatic and oceanic current activity. Geological Society of America Bulletin 121, 134–149. doi:10.1130/B26259.1.

Waight, T.E., Weaver, S.D., Maas, R., Eby, G.N., 1998a. French Creek Granite and Hohonu Dyke Swarm, South Island, New Zealand: Late Cretaceous alkaline magmatism and the opening of the Tasman Sea. Australian Journal of Earth Sciences 45, 823–835.

Waight, T.E., Weaver, S.D., Muir, R.J., 1998b. Mid-Cretaceous granitic magmatism during the transition from subduction to extension in southern New Zealand: a chemical and tectonic synthesis. Lithos 45, 469–482.

Walter, M., 1998. Melting of garnet peridotite and the origin of komatiite and depleted lithosphere. Journal of Petrology 39 (1), 29–60.

Weaver, S.D., Smith, I.E.M., 1989. New Zealand intraplate volcanism. In: Johnson, R.W., Knutson, J., Taylor, S.R. (Eds.), Intraplate volcanism in eastern Australia and New Zealand. Cambridge University Press, pp. 157–188. Chapter 4.

Weaver, S.D., Storey, B.C., Pankhurst, R.J., Mukasa, S.B., DiVenere, V.J., Bradshaw, J.D., 1994. Antarctica–New Zealand rifting and Marie Byrd Land lithospheric magmatism linked to ridge subduction and mantle plume activity. Geology 22, 811–814.

Wessel, P., Smith, W.H.F., 1995. New version of the Generic Mapping Tool released, EOS Trans. AGU, p. 329.

Zindler, A., Hart, S., 1986. Chemical geodynamics. Annual Review of Earth and Planetary Sciences 14, 493–571.

Please cite this article as: Timm, C., et al., Temporal and geochemical evolution of the Cenozoic intraplate volcanism of Zealandia, Earth-Science Reviews (2009), doi:10.1016/j.earscirev.2009.10.002